Basin Research (2006) **18**, 277–299, doi: 10.1111/j.1365-2117.2006.00296.x

Lithospheric bulge in the West Taiwan Basin

J. Tensi, F. Mouthereau and O. Lacombe

Laboratoire de Tectonique, UMR 7072, UPMC, Paris Cedex, France

ABSTRACT

We use well data to investigate the timing and the origin of the lithospheric bulge in the West Taiwan Basin. The possibility that the subsidence patterns observed since Middle-Upper Miocene are simply related to the flexural response of the Chinese continental margin to loading is examined by the reconstructions of the West Taiwan Basin evolution using two-dimensional geometric and numerical flexural modelling of a purely elastic plate. Reconstructions of the forebulge and basin evolution since Middle Miocene are finally discussed in terms of plate strength and geological context. The results are finally placed in the framework of the geodynamic setting of the Philippines Sea Plate/Eurasia convergence in order to provide new insights on the early stage of the Taiwan arc-continent collision. Modelling suggests that the initiation of the flexure in the West Taiwan Basin occurred at *ca*. 12.5–8.6 Ma. A good fit is obtained for T_e of 10–20 km, consistent with earlier studies. During 5–6 m year^{-1} the growth of the bulge was static and associated with increasing plate curvature. Then, at 3–4 Ma the bulge migrated forelandward within the West Taiwan Basin in relation to the migration of the load and the increase in plate curvature. The passage of the forebulge into an inherited weaker portion of the Chinese margin produced an increase in plate curvature and renewed extension, leading to enhancement of the bulge uplift and to its localization for a prolonged period of time. Taking into account the age of the flexure initiation and plate convergence rates, we infer that the load might not be related to the arc-continent collision. We conclude that a Middle Miocene obduction, already proposed by some authors, may explain the deflection of the Chinese margin at that time. It is not before 3–4 Ma that the bulge and the load propagated forelandward in association with the development of the Taiwan arc-continent collision.

INTRODUCTION

Foreland basins and adjacent upwarp, the forebulge, form in compressional settings by the flexure of the lithosphere in front of advancing thrust-fold belts (e.g., Watts, 2001; Allen & Allen, 2005). More generally, pro-foreland basin systems (DeCelles and Giles, 1996) develop under a combination of orogenic or surface loads and subcrustal loads, e.g., slab pull. Although exceptions may exist, many of these foreland basins show an initially slow subsidence on basin margin that progressively increases over time. In association with plate flexure, basin margin unconformities in foreland basins have been attributed to forebulge migration by many authors (e.g., Jacobi, 1981; Watts, 1989; Sinclair *et al*., 1991). Such unconformities are characterized by (1) progressive onlaps of the unconformity by synorogenic siliciclastic sediments, (2) onlaps subparallel to the thrust front but oblique to the passive margin, (3) sediments above the unconformity showing a deepening-upward sequence and (4) an erosive zone that is parallel to the orogen and migrated forelandward over time in front of advancing orogenic wedge (Crampton & Allen, 1995).

The recognition and study of forebulge unconformities in foreland basin is important as it provides constraints on plate strength, migration rates of the orogenic wedge, denudation and loading history. However, as noticed by Crampton & Allen (1995), the recognition of forebulge unconformities is often obscured by independent parameters including lateral changes in the flexural rigidity of the plate both along strike and across strike, variations in orogenic advance rate as the continental basement is involved in deformation, changes in the shape in the orogenic wedge and sediment filling of the basin that tend to remove the forebulge by spreading the applied load over a wider area.

Some exceptions of forebulges exist, which do not exhibit diachronous migration such as the Barrow Arch, Alaska (Coakley & Watts, 1991). Theoretical modelling indicated that inelastic yielding in the lithosphere produces weak zones in the foreland that could localize uplift for prolonged periods (Waschbush & Royden, 1992). Also, stress relaxation in a viscoelastic lithosphere produces inward migration of the bulge, which may explain the stratigraphic architecture in the Appalachian foreland basin (Quinlan & Beaumont, 1984). In association with forebulges, shallow normal faulting is often reported in continental foreland basins (e.g., Lorenzo *et al*., 1998; Ussami *et al*., 1999).

The western foreland of the still active Taiwan collision belt has been primarily investigated in the work of Covey (1986). Approximately 5000 m of siliciclastic sediments derived from the orogen were deposited during the Pliocene–Pleistocene. Recently, several studies attempted to

Correspondence: F. Mouthereau, Laboratoire de Tectonique, UMR 7072, UPMC, 4 Place Jussieu, 75252 Paris Cedex 05, France. E-mail: frederic.mouthereau@lgs.jussieu.fr.

characterize the present geometry of the West Taiwan foreland basin, including the position of the forebulge and the characterization of the forebulge unconformity (Yu & Chou, 2001). Some other works, using gravity data, placed constraints on the plate rigidity and on the origin of loading (Lin & Watts, 2002; Mouthereau & Petit, 2003). For instance, lateral variations of the plate rigidity were proposed along the strike of the Taiwan foreland (Mouthereau & Petit, 2003). These mechanical variations were found in close geographical relationships with structural heterogeneities inherited from the rifting episodes. Weaker portions of the lithosphere are observed over areas adjacent to margin promontories that suffered enhanced erosion due to pronounced uplift. In contrast, stronger areas are localized in reentrants that contain a nearly complete stratigraphic record. Despite the work of Wang (2001), who attributed some characteristics of the subsidence patterns in the basin to plate flexure in the upper Miocene, there were few attempts to reconstruct the evolution of the plate flexure through time.

The aim of this study is to take advantage of the numerous available well data along the strike of the West Taiwan Basin to examine the timing and the origin of the lithospheric bulge. More generally, we examine the possibility that the observed subsidence pattern in the basin, since Middle-Upper Miocene, simply relates to the flexural response of the Chinese margin to loading. All available well-based and outcrop-based data are combined in order to provide a comprehensive stratigraphic scale of the Neogene formations in the West Taiwan Basin. One-dimensional Airy-type backstripping is then used to perform two-dimensional (2D) reconstructions of the evolution of the plate flexure over time using 2D geometric and numerical flexural modelling of a purely elastic plate. We specifically examine what combination of loads and elastic thickness through time provides the best explanation of the observed subsidence pattern. Reconstructions of the forebulge and basin evolution since Middle Miocene are finally discussed in terms of plate strength and geological context. To this aim, we rely upon the recent works dealing with the rigidity of the Chinese margin in the Taiwan area (Lin & Watts, 2002; Mouthereau & Petit, 2003). Ultimately, the results will be placed in the framework of the geodynamic setting of the Philippines Sea Plate/Eurasia convergence in order to provide new insights on the early stage of the Taiwan arc-continent collision.

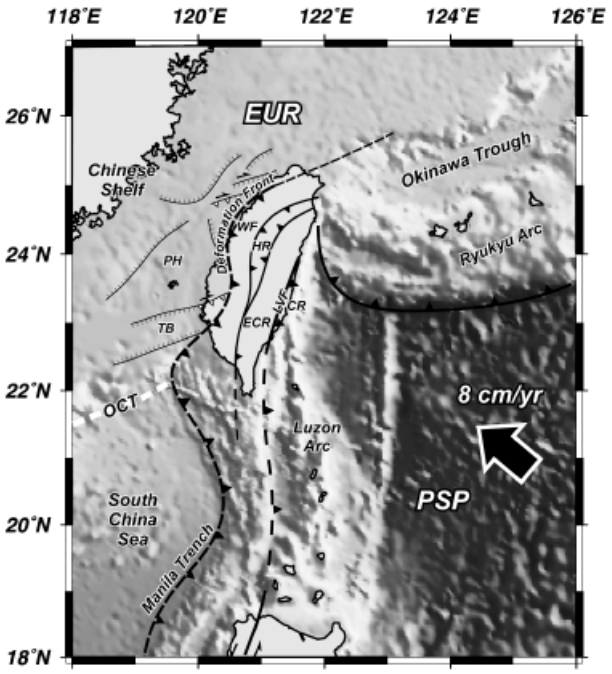

Fig. 1. Geodynamical setting of the Taiwan arc-continent collision. The main inherited Paleogene extensional basins (e.g. Tainan Basin) and basement highs (Peikang High and Kuanyin High) are depicted in the West Taiwan Basin. WF, Western Foothills; HR, Hsuehshan Range; ECR, Eastern Central Range; CR, Coastal Range; TB, Tainan Basin; PH, Peikang High; KH, Kuanyin High; LVF, Longitudinal Valley Fault; OCT, Ocean-Continent transition.

FROM RIFTING TO COLLISION: SOME REMARKS ON THE TECTONIC HISTORY OF THE CHINESE CONTINENTAL MARGIN

Geological background

The Taiwan Mountain Belt (Fig. 1) is a fold-and-thrust belt that developed into the Chinese continental margin as a result of the convergence between the Eurasian plate and the Philippine Sea plate (Suppe, 1980, 1981, 1984; Ho, 1986). The current plate convergence velocity of the Philippine Sea plate relative to Eurasia is about 7–8 cm year^{-1} (Seno *et al*., 1993; Yu *et al*., 1997). Its structure is summarized in Figs 2 and 3a. To the East, the Coastal Range represents that part of the Luzon Arc accreted onto the Eurasian continental margin. Miocene volcanic rocks and intra-arc flyschs basins are recognized in the Coastal Range. The suture zone, which separates the Coastal Range from rocks belonging to the Eurasian margin, is outlined by a narrow depression, the Longitudinal Valley where the active Longitudinal Valley Fault occurs (Tsai, 1986; Lee, 1994). The Longitudinal Valley is flanked to the West by the Eastern Central Range in which the Mesozoic basement of the Chinese margin is exposed at about 2000 m above sea level. The Hsüehshan Range is essentially composed of slightly metamorphosed slates of depositional Palaeogene age. It is interpreted as a Palaeogene trough inverted during the Neogene (Lee *et al*., 1997).

Several conceptual geodynamical models based on plate reconstructions placed constraints on the Neogene evolution of the Taiwan collision. One can tentatively divide these models into two groups. The first category of models supports the hypothesis of a single collision event between the Luzon Arc and the Eurasian continental margin (Suppe, 1984; Barrier & Angelier, 1986; Teng, 1990, 1996; Huang *et al*., 1997; Lallemand *et al*., 2001; Malavieille *et al*.,

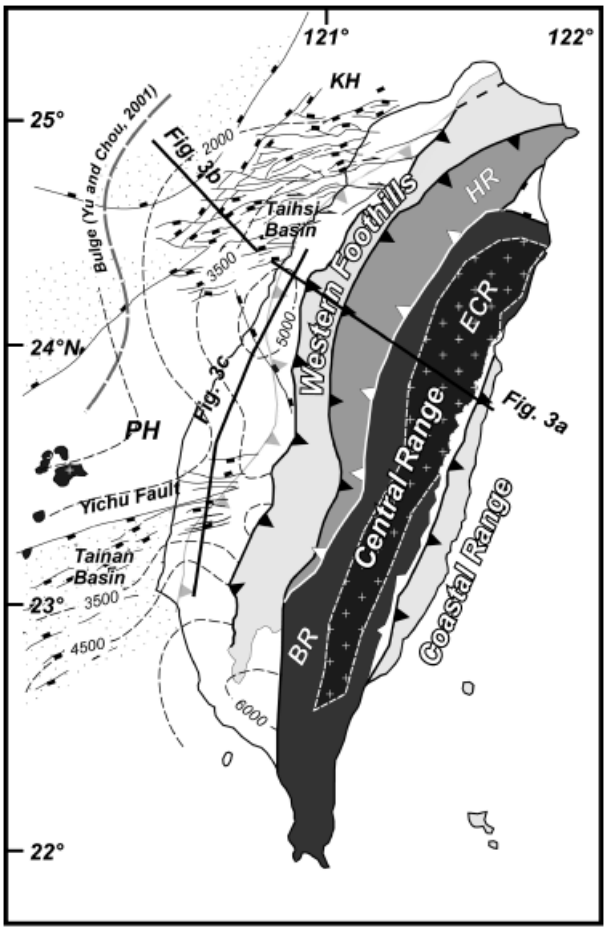

Fig. 2. Geology of the Taiwan fold-thrust belt and its foreland. The Peikang basement high, the Taihsi Basin and the Tainan Basin outline the pre-orogenic structural inheritance of the Chinese passive margin. Also, the main thrust sheet units that form the orogenic wedge are shown such as the Western Foothills, the Hsuehshan Range (HR), Backbone Range (BR), the Central Range including the Eastern Central Range (ECR) and the Coastal Range. The position of the current flexural bulge determined by Yu & Chou (2001) is also shown.

2002; Sibuet & Hsu, 2004). However, the age of the collision onset is still controversial as it ranges from 12 up to 2 Ma for some authors. The second set of models interprets the existence of diachronous sedimentary unconformities and tectonic mélanges as the result of a two-stage collision at 8 and 3 Ma (Chang & Chi, 1983; Huang, 1984; Lu & Hsü, 1992; Delcaillau *et al*., 1994) or obduction at 14–13 Ma, followed by a collision event at 8 Ma (Pelletier & Stephan, 1986). It is clear based on this brief review that the early stages of the collision are still poorly understood.

Palaeogene pre-orogenic history of the Chinese continental margin

The Early Cenozoic history of the Chinese continental margin was dominated by the opening of the South China Sea (Figs 1 and 2). On the Chinese continental margin, the base of syn-rift deposition is dated 60–55 Ma (Clift & Lin, 2001; Lin *et al*., 2003). These Palaeogene syn-rift sediments were slightly metamorphosed during the collision and now form part of the Hsuehshan Range (Fig. 2). They are unconformably overlain by post-rift Oligo-Miocene deposits. Subsurface data and stratigraphic constraints in the Pearl River Mouth Basin place the cessation of extension on the South China Sea Margin at ~28 Ma at ODP site 1148 (Clift *et al*., 2001), thus providing an age estimate for the initiation of continental break-up. Offshore data rather indicate that the continental rifting ceased by ~24 Ma in the entire south-east China margin (Clift & Lin, 2001; Lin *et al*., 2003). Interpretations of magnetic anomalies reported in the South China Sea place the start of spreading during anomaly 11, i.e. ~30 Ma (Taylor & Hayes, 1980; Briais *et al*., 1993), shortly before the cessation of extension. The youngest magnetic anomalies found in the South China Sea reveal that the spreading of the Eurasian oceanic lithosphere ceased at 16 Ma. Following the cessation of spreading, a later extensional episode caused reactivation of older normal faults and minor subsidence at ~12–14 Ma (Clift & Lin, 2001).

Geological data and plate reconstructions further suggest age concordance between the cessation of the spreading in the South China Sea and the collision of the North Palawan-Mindoro continental block with the Philippines archipelago (Holloway, 1982; Taylor & Hayes, 1983; Hall, 2002).

The Western Taiwan Basin

The accretion of thrust units onto the Chinese margin during the Neogene has resulted in shortening and thickening of the mountain belt, producing loading required to flex the Eurasian lithosphere. As a result, a foreland basin system developed in Western Taiwan at the front of the Taiwan mountain belt. It is divided into a foreland fold-thrust belt or wedge-top depozone (DeCelles & Giles, 1996), the Western Foothills and a foredeep, the Coastal Plain. Both involve Neogene synorogenic deposits that are actively folded and faulted at the orogenic front (Figs 2 and 3a). Beyond the thrust front, the current foredeep basin extends offshore in the Taiwan Strait.

The acquisition and processing during the past 30 years, by the Chinese Petroleum Corporation, of seismic-reflection profiles calibrated with geophysical logging have allowed the recognition of a major unconformity at the base of the foreland basin sequences in the Western Taiwan basin (Fig. 3b) (Yu & Chou, 2001; Lin *et al*., 2003). These data further helped to draw the current position of the forebulge (Yu & Chou, 2001) beneath the Taiwan Strait (Fig. 3b). Using four well-based sections distributed along the strike of the basin, Yu & Chou (2001) noticed that the stratigraphic gap across the unconformity increases over 50 km from the thrust front towards the forebulge. Figure 3b shows that the passive margin strata are onlapped progressively forelandward by younger Neogene sediments. This confirms that the unconformity observed on seismic profiles is a forebulge unconformity that developed in front of the advancing orogenic wedge. This unconformity is caused by

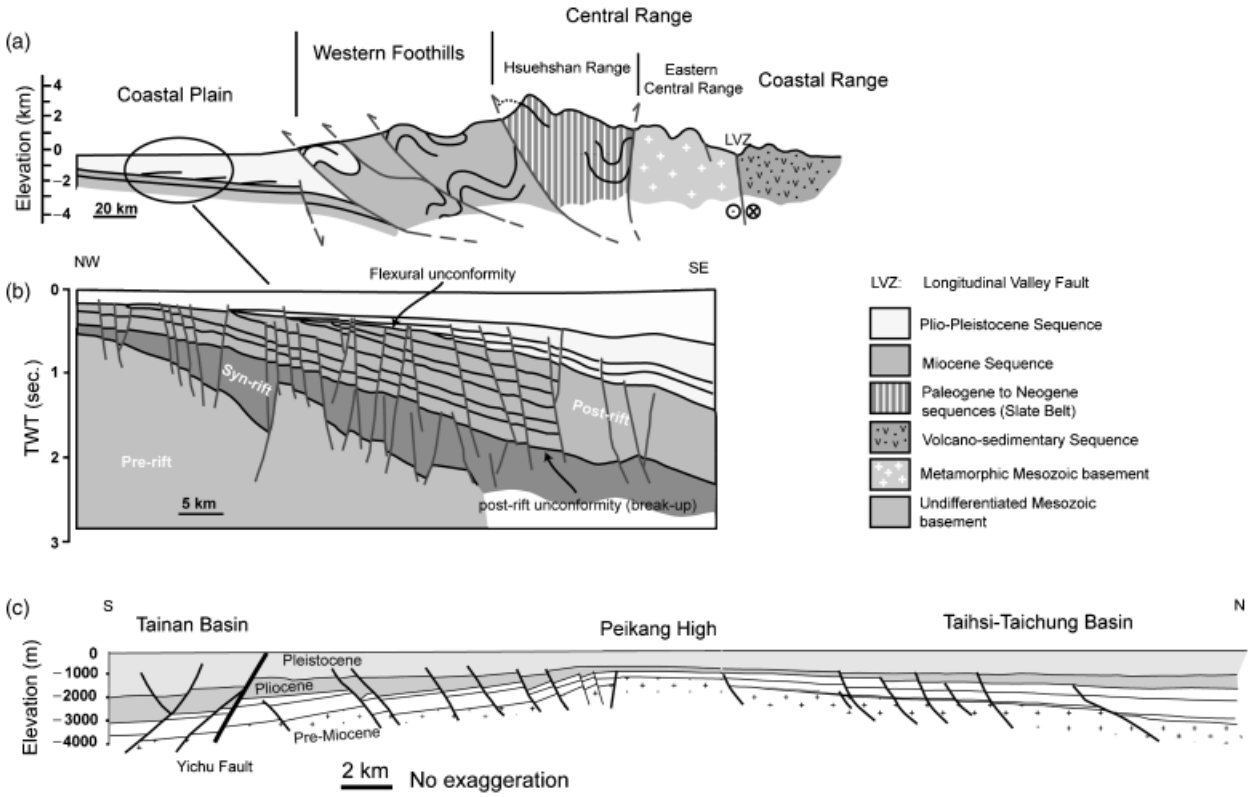

Fig. 3. Subsurface structure of the western foreland of Taiwan and its forebulge unconformity. (a) General cross-section of the Taiwan fold-thrust belt. (b) NW-SE line-drawing in the western foredeep based on the seismic reflection profile performed by the Chinese Petroleum Corporation (Yu & Chou, 2001) showing the onlaps of the Neogene deposits above the forebulge unconformity. Note that the most recent part of the Pleistocene sediments is spread over the bulge, thus defining an important stratigraphic gap between the Early Miocene and Pleistocene strata. Further to the east, i.e., within the Western Foothills, this unconformity is expected to be older. Note also the presence of reactivated normal faults during the Plio–Pleistocene. (c) N-S line-drawing along the strike of the foredeep (unpublished data from the Chinese Petroleum Corporation) showing the Peikang basement promontory and adjacent Tainan and Taichung basins. Note the south-facing Yichu normal fault bounding the Tainan Basin.

the erosion of the passive margin strata as the lithospheric bulge passed into the basin. Below the unconformity, the truncated syn-rift and post-rift sedimentary sequences of the passive margin are clearly observed (Fig. 3b).

Offshore, in the Taihsi basin (Fig. 2), an age of 6.5 Ma has been proposed for the base of foreland strata, which lies between the Kueichulin Formation and the Nanchuang Formation (Lin *et al*., 2003). Onshore, 40–50 km eastward from the previous point, in the fold-and-thrust belt of the Western Foothills, field data showed for years the occurrence of an upper Miocene unconformity between the shallow-marine Kueichulin Formation and the Nanchuang Formation (Chou, 1971; Tang, 1977; Chinese Petroleum Corporation, 1982; Ho, 1988). Based on biostratigraphy, this unconformity seems slightly older ~8.6 Ma.

Sedimentological data also provide important constraints of the evolution of the foredeep. The sedimentary facies in the Taiwan foredeep are largely dependent on the position of basins and highs inherited from the Palaeogene extension and on the bathymetric profile across the continental margin, which is controlled by the position of the continental-ocean transition to the south (Figs 1 and 3c) (Ho, 1986). Although important changes in sediment facies may occur along strike due the inherited bathymetry of the Chinese margin, we attempt hereafter to summarize the main trends. For instance, the Lower Miocene Talu Formation (Ho, 1988) of the Nankang Group is composed of post-rift turbiditic sequences (Fig. 4). The reconstruction of palaeocurrents in this formation reveals that these silicilastic deposits were supplied from the North, i.e.,

Fig. 4. Lithofacies and biostratigraphy of the Neogene formations based on well data and outcrop-based data in the Coastal Plain and the Western Foothills (see text for the references of published data used to perform this compilation). Log sites are established from North to South (from left to right and top to bottom). Specifically, the main stratigraphic gap between the Nanchuang Formation (completely lacking sometime, e.g., well PKS-1) and the overlying transgressive sequence of the Kueichulin Formation is shown. This unconformity represents the forebulge unconformity. Owing to the deeper sedimentary environment, and continuous sedimentation to the South of the foredeep such as in Tainan area and in well PTG-1, this unconformity is less clear. Sedimentary structures and ichnofacies used to determine the palaeo-bathymetries are shown. Evidence of clasts running from the orogen and palaeo-current directions is also indicated. Magnetostratigraphy performed in the Plio–Pleistocene strata is indicated.

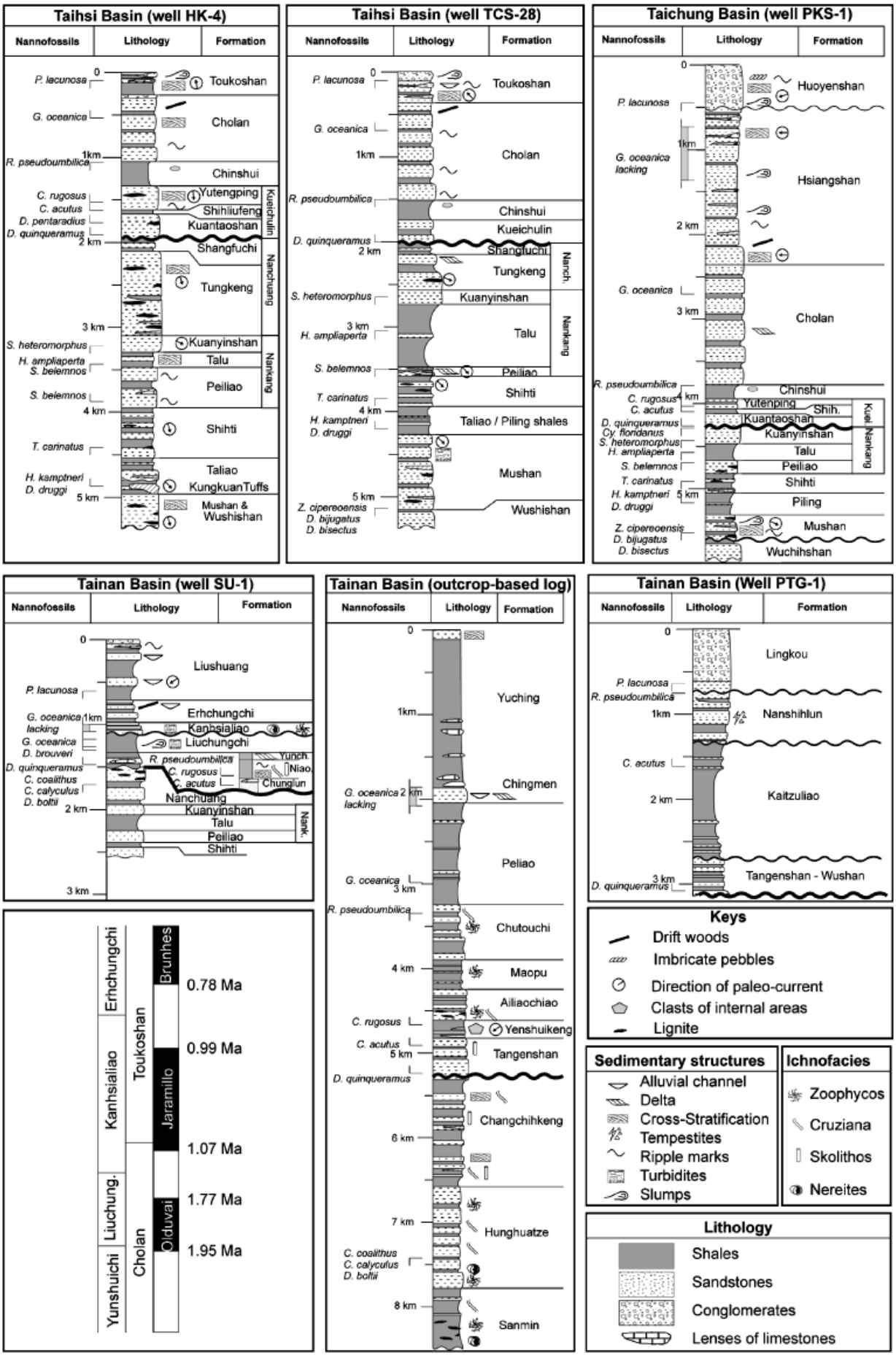
Taihsi Basin (well HK-4)
Nannofossils
Lithology
Formation
P. lacunosa
G. oceanica
R. pseudoumbilica
C. rugosus
C. acutus
D. pentaradius
D. quinqueramus
S. heteromorphus
H. ampliaperta
S. belemnos
T. carinatus
H. kamptneri
D. druggi
Toukoshan
Cholan
Chinshui
Yutengping
Shihliufeng
Kueichulin
Kuantaoshan
Shangfuchi
Nanchuang
Tungkeng
Kuanyinshan
Talu
Nankang
Peiliao
Shihti
Taliao
KungkuanTuffs
Mushan & Wushishan
Taihsi Basin (well TCS-28)
Nannofossils
Lithology
Formation
P. lacunosa
G. oceanica
R. pseudoumbilica
D. quinqueramus
S. heteromorphus
H. ampliaperta
S. belemnos
T. carinatus
H. kamptneri
D. druggi
Z. cipereoensis
D. bijugatus
D. bisectus
Toukoshan
Cholan
Chinshui
Kueichulin
Shangfuchi
Nanch.
Tungkeng
Kuanyinshan
Talu
Nankang
Peiliao
Shihti
Taliao / Piling shales
Mushan
Wushishan
Taichung Basin (well PKS-1)
Nannofossils
Lithology
Formation
P. lacunosa
G. oceanica lacking
G. oceanica
R. pseudoumbilica
C. rugosus
C. acutus
D. quinqueramus
Cy. floridanus
S. heteromorphus
H. ampliaperta
S. belemnos
T. carinatus
H. kamptneri
D. druggi
Z. cipereoensis
D. bijugatus
D. bisectus
Huoyenshan
Hsiangshan
Cholan
Chinshui
Yutenping
Shih.
Kuantaoshan
Kuanyinshan
Talu
Peiliao
Shihti
Piling
Mushan
Wuchihshan
Kueichulin
Nankang
Tainan Basin (well SU-1)
Nannofossils
Lithology
Formation
P. lacunosa
G. oceanica lacking
G. oceanica
D. brouweri
D. quinqueramus
C. coalithus
C. calyculus
D. boltii
R. pseudoumbilica
C. rugosus
C. acutus
Liushuang
Erhchungchi
Kanhsialiao
Liuchungchi
Yunch.
Niao.
Chunglun
Nanchuang
Kuanyinshan
Talu
Peiliao
Shihti
Nank.
Tainan Basin (outcrop-based log)
Nannofossils
Lithology
Formation
G. oceanica lacking
G. oceanica
R. pseudoumbilica
C. rugosus
C. acutus
D. quinqueramus
C. coalithus
C. calyculus
D. boltii
Yuching
Chingmen
Peliao
Chutouchi
Maopu
Ailiaochiao
Yenshuikeng
Tangenshan
Changchihkeng
Hunghuatze
Sanmin
Tainan Basin (Well PTG-1)
Nannofossils
Lithology
Formation
P. lacunosa
R. pseudoumbilica
C. acutus
D. quinqueramus
Lingkou
Nanshihlun
Kaitzuliao
Tangenshan - Wushan
Erhchungchi
Kanhsialiao
Liuchung.
Yunshuichi
Toukoshan
Cholan
Brunhes
Jaramillo
Olduvai
0.78 Ma
0.99 Ma
1.07 Ma
1.77 Ma
1.95 Ma
Keys
Drift woods
Imbricate pebbles
Direction of paleo-current
Clasts of internal areas
Lignite
Sedimentary structures
Alluvial channel
Delta
Cross-Stratification
Tempestites
Ripple marks
Turbidites
Slumps
Ichnofacies
Zoophycos
Cruziana
Skolithos
Nereites
Lithology
Shales
Sandstones
Conglomerates
Lenses of limestones

from the Chinese continental margin (Chou, 1980). These sediments are overlain during the Middle Miocene by shallower deposits of the Nanchuang Formation comprising white sandstones and coal-bearing rocks of the Shangfushi Formation. In some places of the West Taiwan Basin, the Nanchuang Formation is incised or completely missing across the margin unconformity described above. This relative sea-level fall is assumed to be associated with the passage of the forebulge uplift into the passive margin. During the deposition of the Nanchuang Formation, the direction of palaeocurrents changed from southeastward to southward (Chou, 1980). This change reveals the development of a trough whose orientation becomes oblique to the ENE-trending Chinese margin but parallel to the trend of the Taiwan orogen. This episode is followed by the deposition of a transgressive sequence of the Kueichulin Formation. These siliciclastic deposits correspond to shallow-marine deltaic and tidal sediments deposited above the basin unconformity. The relative sea-level rise associated with these deposits reveals the drowning of the N-S depression. Southward, the Kueichulin Formation laterally passes to offshore turbiditic sequences of the Lower Gutingkeng Formation.

Thrusting is known to be active in the Western Foothills since 4–5 Ma (e.g., Mouthereau *et al.*, 2001). The activity of the thrust front is coeval with the sedimentation of a thick shallowing-upward sequence of Plio–Pleistocene marine to fluvial sands and conglomerates (1–2 km) in the West Taiwan Basin (Ho, 1986). Reworked fossils and the orientation of palaeocurrents in the Chinshui Formation confirm that the basin was fed from the East at that time, i.e., from the growing orogen (Covey, 1986).

To summarize, a major basin unconformity is recognized in the stratigraphic record of the West Taiwan Basin. The stratigraphic gap across this unconformity increases forelandward and the deposits above the unconformity show a deepening-upward sequence. This reveals strong similarities with the characteristics of forebulge unconformities (Crampton & Allen, 1995) in the early underfilled stage of foreland basins (Sinclair, 1997).

SUBSIDENCE AND PLATE FLEXURE ANALYSES

Stratigraphy of the neogene strata in the Western Foreland

The available stratigraphic data are derived from 101 wells published by the Chinese Petroleum Corporation and outcrop-based studies (Chou, 1971; Chou, 1976; Yeh, 1987; Ting *et al.*, 1991; Hong, 1997). Together with earlier syntheses (Chou, 1980; Covey, 1986; Ho, 1986, 1988), these data are combined to propose an updated stratigraphic synthesis of the Western Taiwan foreland basin (Fig. 4). Practically, biostratigraphic data are combined with radiometric and magnetostratigraphic data when available. This compilation is shown in Fig. 5.

The earliest biostratigraphic works in Taiwan reported very few reference biomarkers, especially for the Pliocene

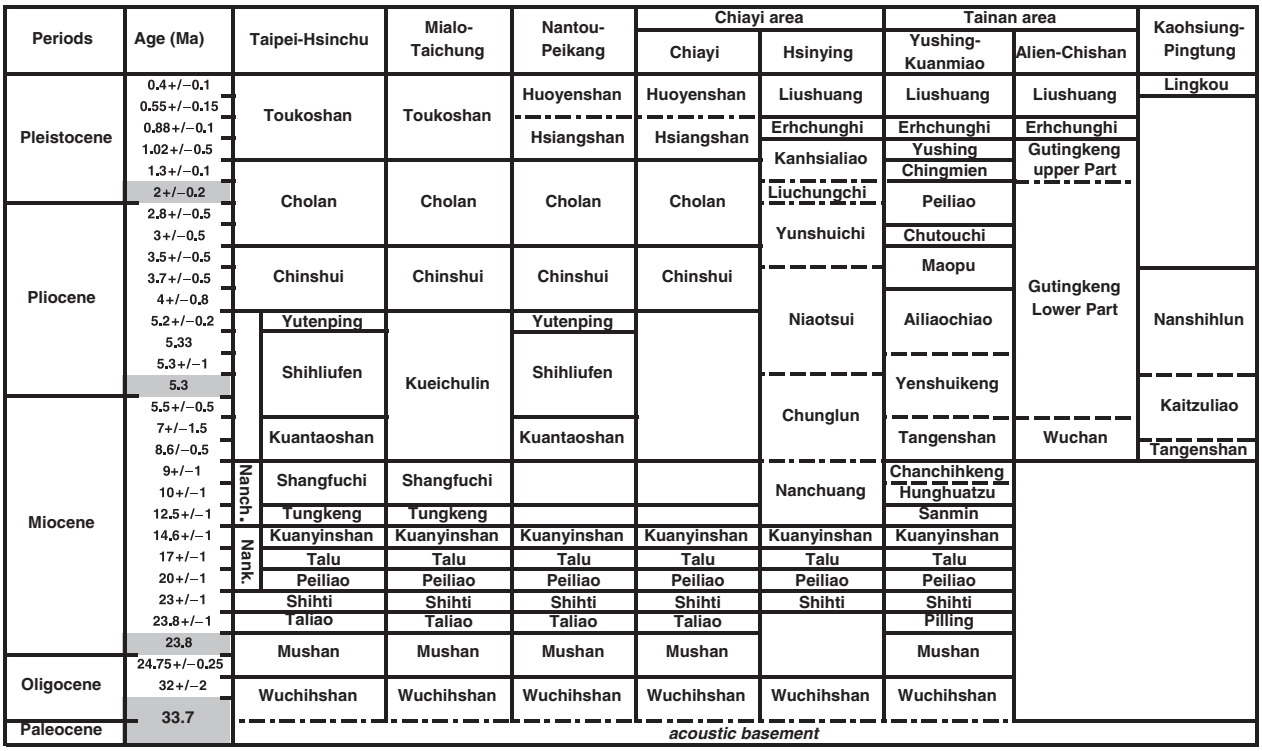

Fig. 5. Stratigraphy of the Neogene sediments within the West Taiwan Basin used in this study (see text for references). As ages were determined based on biostratigraphic constraints, especially nanoplankton, they depend on the first and the last occurrences of taxons shown in Fig. 4. This compilation is consistent with recent studies (Lin *et al.*, 2003).

(Oinomikado, 1955). The current foraminiferal biostratigraphy in Taiwan mainly relies on the syntheses performed by Chang (1975) and Huang (1968, 1976). The results of these studies were compared with other nanofossil syntheses (Chi, 1978; Huang, 1978; Chang & Chi, 1983) revealing fair levels of consistency between both approaches, especially at the Oligocene/Miocene and Miocene/Pliocene boundaries. In contrast, the Pliocene/Pleistocene boundary determined from foraminifers and nanoplanktons differs. Along the strike of the West Taiwan Basin, the first occurrence of foraminiferal taxon used to define the Pliocene/Pleistocene boundary (*Globorotalia truncatulinoides*) is diachronous with respect to the Olduvai magnetic event that is synchronous by nature (see the discussion in Chi, 1978). In contrast, the first occurrence of nanofossils (i.e., *G. oceanica*) seems to be synchronous with respect to the Olduvai event. Therefore, regarding the Pliocene/Pleistocene boundary, nanofossils were preferred in the present study. Note also that foraminifers are more sensitive to environmental conditions (especially to latitude variation) than nanofossils and are often missing from well data information. The occurrences and palaeomagnetic events used in the study are indicated in Fig. 4.

We have adopted the chronostratigraphic compilation of Berggren *et al.* (1995) as it takes into account both the results of the cyclostratigraphy (based on rythmicity of orbital parameters) and corrections in radioactive constants. The magnetostratigraphic study of Chen *et al.* (2001) also provides helpful information for the last 2 Ma. It is worth noting that the stratigraphic synthesis in Fig. 5 involves strong, albeit reasonable assumptions. Two main hypotheses remain: strict equivalence between first/last occurrences and first/last appearances of biostratigraphic taxons.

Based on the biostratigraphic compilation shown in Fig. 5, we suggest an age of 8.6 Ma for the base of the Kueichulin Formation. Because the Kueichulin Formation lies above the foreland basin unconformity, we suggest that at its minimum hiatus, i.e. in internal part of the basin, the unconformity might be as old as 8.6 Ma. An age of 8.6 Ma may be consistent with younger ages of $\sim$6.5 Ma for the unconformity proposed offshore (Lin *et al.*, 2003) if we keep in mind that the forebulge unconformity is basically diachronous and especially younger towards the foreland.

Airy-type backstripping and the deflection of the lithosphere

Backstripping is a commonly used method that attempts to isolate the origin of the subsidence recorded by sediments in the basin (Steckler & Watts, 1978). In this technique, the effect of the decompacted stratigraphic column at each time step is removed (backstripped) and then replaced by water, and the depth of the basement is calculated. One-dimensional backstripping assumes that the lithosphere responds to loads by local Airy-type loading. One problem with the Airy approach is that the estimate of tectonic subsidence/uplift is limited to the vicinity of well sites. This is why 2D flexural backstripping (e.g., Thorne & Watts, 1989), which takes into account plate rigidity, is generally preferred and more suitable for large areas. In the case of Taiwan, the available wells in the foreland cover a sufficiently wide area from the fold-thrust belt to the bulge. Hence, there is no need for extrapolation. As a consequence, we assume that Airy-type backstripping is a reasonable approach to investigate the subsidence patterns in the West Taiwan Basin.

In addition to the effects of the sedimentary load, palaeobathymetry and eustasy have also been taken into account. The tectonic subsidence Z for local isostasy is given by Steckler & Watts (1978):

$$Z = S^* \frac{(\rho_m - \rho_{si})}{(\rho_m - \rho_w)} + W + \frac{\Delta_{abs}\rho_m}{(\rho_m - \rho_w)}$$
$$\text{with } \rho_{si} = \frac{\sum_{i=1}^{n} (\rho_w \phi_i + \rho_i(1-\phi_i))S_i^*}{S^*}$$

where S^* is the decompacted thickness of sedimentary column, W is the palaeobathymetry at which the sediment was deposited in the time interval considered, $\rho_{mantle} = 3330\,kg\,m^{-3}$ and $\rho_{water} = 1030\,kg\,m^{-3}$ are the densities of mantle and water, respectively, and ρ_{si} the average density of the ith column. Δ_{abs} is the eustatic correction that refers to the global oscillations of sea level. We use sea-level corrections based on the chart proposed by Haq *et al.* (1987).

Understanding the response of the continental passive margin to loading from well data requires our ability to fit the foreland basin geometry, defined by the geometry of the decompacted depths to foreland basement, by a theoretical deflection profile. For this purpose, in a first type of models, we seek to fit the data by a simple geometric model. The shape of the Chinese margin at different time steps was ascertained by using decompacted sediment columns along a given profile. The 2D deflection is obtained by downflexing a passive margin reference layer following the universal deflection profile described in Turcotte & Schubert (2002) for a purely elastic plate that bends under a line load. Note that the reconstructed profiles implicitly assume a broken plate model with moment and line loads applied at the plate end.

In a second type of models, we evaluate the role of bending moments in producing the observed forebulge and basin evolution. Indeed, in the absence of reliable constraints on the shape of the load through time, the plate deflection is calculated numerically for loads represented by variable bending moments. Bending moments are assumed to represent the sum of the interaction with another plate and the effects of distributed loads acting on the plate from above and below. The plate is a fractured plate and its rheology is simplified to a purely elastic plate. The assumption of a broken plate is supported by the subduction context.

The general equation of the deflection of a plate is thus given by

$$D\frac{\partial^4 w(x)}{\partial x^4} + T\frac{\partial^2 w(x)}{\partial x^2} + kw(x) = 0 \qquad (1)$$

where $D = ET_e^3/(12(1-\nu^2))$ is the rigidity of the lithosphere, T_e is the elastic thickness with E and ν are the Young's modulus and Poisson's ratio, respectively, T represents the horizontal forces applied at the plate end, k is the restoring force proportional to the difference between mantle ($\rho_{mantle} = 3330\,kg\,m^{-3}$) and infill densities and the acceleration of the gravity, w is the deflection and x is the horizontal distance along the coordinate axis (Turcotte & Schubert, 2002). Because the horizontal forces have generally little effect on the first-order evolution of the flexure (e.g., Crampton & Allen, 1995), T is set to zero in all models. Moreover, we assume in all models that water infills the flexural depression, so that $\rho_{infill} = \rho_{water} = 1030\,kg\,m^{-3}$.

The deflection profile for plate flexure is obtained by solving numerically Eqn. (1) using central finite differences and back substitution in a five-band matrix following boundary conditions for a semi-infinite or a broken plate as described in Sheffels & McNutt (1986). At the edge of the plate ($x = 0$), where the deflection is maximum, the applied load is modelled by variable bending moments $M = -D(\partial^2 w/\partial x^2)_{x=0}$ (positive for counterclockwise) that are assumed to represent a combination of surface and subsurface loads in the vertical and horizontal directions. Moreover, no shear (free edge) is assumed at $x = 0$ so that $D(\partial^3 w/\partial x^3)_{x=0} = T(\partial w/\partial w)_{x=0} = 0$. At the opposite side of the plate, the deflection is zero $w(\infty) = 0$ and $\partial w/\partial x = 0$. The plate deflection and distributed load is discretized into 400 nodes spaced every 5 km. Erosion of the growing orogen and sedimentation in the basin using diffusion equations can be included in the algorithm (Flemings & Jordan, 1989; Sinclair *et al.*, 1991) but this possibility was not required in the present study.

The current elastic thickness of the Chinese continental margin has already been estimated in recent studies using gravity data (Lin & Watts, 2002; Mouthereau & Petit, 2003). Whatever the rheological properties assumed for the lithosphere, purely elastic for Lin & Watts (2002) or brittle-viscous-elastic for Mouthereau & Petit (2003), these studies showed that the Eurasian plate beneath the West Taiwan Basin is essentially weak with elastic thicknesses close to 13–18 km. We finally assume an elastic thickness of 10–20 km that covers a sufficiently large range of possible values. The base of the foreland basin used in the modelling refers to the decompacted depths of the top of the Talu Formation dated 14.8 Ma.

Compaction corrections

Because of the loss of water during sediment burial, the effect of mechanical compaction may be significant in one-dimensional backstripping. For decompaction, the empirical porosity-depth curves for different lithologies are usually used (Bond & Kominz, 1984). Taking into account the uncertainties of porosity for a single lithology, it is usually reasonable to decompact the sedimentary column using a simple averaged depth–porosity curve regardless of lithologies. The evolution of the rock porosity, φ, with depth, z, follows an exponential law $\phi = \phi_0 e^{-cz}$, where ϕ_0 describes the surface porosity of rocks and c is the coefficient of compaction (Table 1).

Table 1. Values of the porosity of rocks for lithologies observed in the Western Taiwan foreland and compaction coefficient used in this study after Allen and Allen (2005)

Lithology	Surface porosity ϕ_0	Compaction coefficient (km^{-1})	Grain density ($kg\,m^{-3}$)
Shales	0.63	0.51	2720
Sandstones	0.49	0.27	2650
Mudstones	0.56	0.39	2680

Porosity–depth curves reconstructed from available wells in the western basin of Taiwan (Hung *et al.*, 1999; Lin *et al.*, 2003) clearly show that the reduction of porosity is primarily controlled by the presence of shales and their mechanical compaction. However, lithological control of the porosity-depth profile has also been locally suggested (Hung *et al.*, 1999). For instance, over- or under-compaction of rocks is common in areas of high sedimentation rates and shale deposition like Taiwan. The Pleistocene deposits located in the southern Taiwan foreland are characterized by a high sedimentation rate up to $3\,km\,Ma^{-1}$ for the last 1 Ma (Chang & Chi, 1983; Chen *et al.*, 2001), almost twice higher than in other foreland basins (Jordan, 1995). In addition, sandstones, which are abundant in some parts of the western basin, display strong contrasts in porosity because of chemical compaction.

For instance, the lower Miocene Shihti Formation drilled in well KY-1 (Fig. 6a) is under-compacted as indicated by the gain of porosity at a depth of 2 km (Chou, 1976) with respect to a theoretical porosity–depth profile. The low permeability of shales of the Talu Formation above the Shihti Formation stopped the upward flow of water. As a result, the shales of the Talu Formation have supported part of the lithostatic pressure and are thus responsible for the under-compaction observed in the underlying Shihti Formation. In contrast, the Shihti Formation in well HTP-1 is over-compacted (Fig. 6b). Chemical compaction, which often occurs especially under 1.5 km (Schmidt & McDonald, 1979), cannot alone explain the low observed values of porosity. An explanation would be that the Shihti Formation was buried and compacted at greater depths and was then uplifted and/or eroded. The location of well HTP-1 within one of the main folds of the Western Foothills (Namson, 1984; Hung & Wiltschko, 1993) probably provides an explanation for such observations. On the other hand, low porosity values in the Palaeogene strata of wells PK-2, PK-3 and SL-1 may be tentatively explained by Oligocene uplift of the passive margin documented by Lin *et al.* (2003). Because of the lack of available in-situ porosity constraints, we adopted an exponential porosity-depth law with coefficients derived from default lithologies (Table 1).

The decompacted thickness and the average porosity of the sedimentary column over time are obtained using the

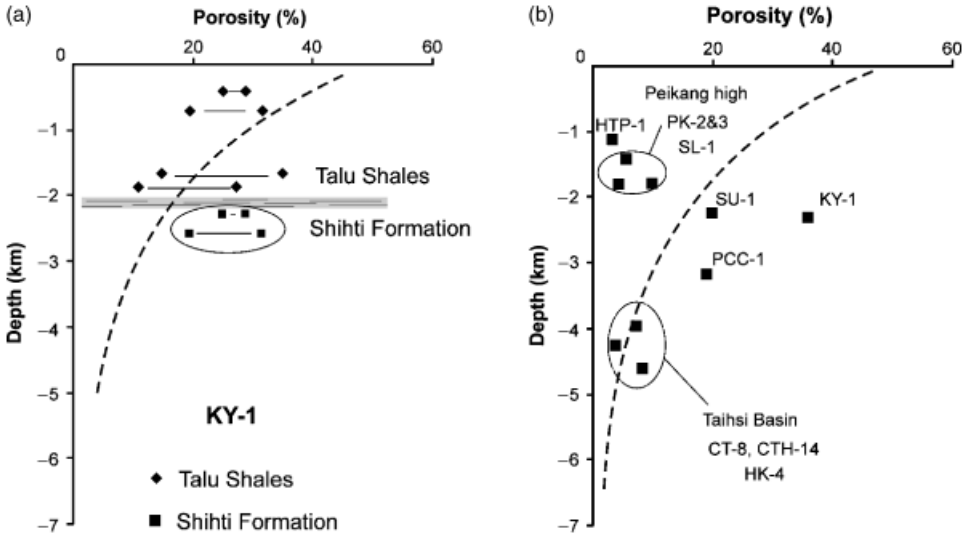

Fig. 6. Examples of under- and over-compaction of the Shihti Formation (sandstones) for some wells of the Taiwan foreland. The theoretical averaged exponential porosity–depth profile is shown as dashed lines. (a) In the KY-1 well (Hsinchu area), impermeability of the shales of the Talu Formation (◆) results in the undercompaction of the underlying Shihti Formation (■). In well HTP-1, the sandstones of the Shihti Formation are undercompacted. Tens of kilometres southward, in wells CT-8, CTH-14, HK-4 this trend is not observed (Hung *et al*., 1999). b) In the vicinity of the Peikang High (PK 2–3 and SL-1), the sandstones of the Shihti Formation are apparently overcompacted relative to their depths. This could be interpreted as the effect of erosion of the overlying strata above the Shihti Formation in relation to the uplift of the Peikang High. In contrast, there porosity follows the theoretical porosity–depth evolution in the Taihsi Basin (CT-8, CTH-14 and HK-4).

simplified method of Angevine *et al*. (1990) based on the method of Van Hinte (1978). After the removal of the top layer, we obtain new porosity values for the decompacted underlying layers following the exponential porosity–depth profile. We assumed that the porosity of a given layer is constant at a depth, which is taken as the half of the layer thickness. As the layers are quite thin, this assumption does not introduce critical errors. By including the effect of eustasy and palaeo-bathymetry, we obtain the total subsidence.

ONSET OF PLATE FLEXURE AND FLEXURAL BULGE DEVELOPMENT

The neogene depocentres

Among the 101 wells available, only 61 have provided sufficient information to be used further in this study (Fig. 7). The wells are distributed onshore and offshore with some concentration in the petroleum basins of the Taihsi Basin, in the Miaoli area to the north and the Tainan Basin to the south of the Peikang promontory. Figure 8 shows that the West Taiwan Basin is deepening southwards regardless of the time period considered, Miocene, Pliocene or Pleistocene. This is a direct consequence of the orientation of the shelf break oblique to the trend of the orogen and located to the south of the Tainan Basin (Figs 1 and 3b).

Figure 8a presents an isopach map of the Miocene deposits. A significant sediment accumulation is observed between the Taihsi Basin and the Peikang promontory. This depocentre is bounded by N60°E-trending fault zones, which are parallel to the orientation of the rifted continental margin. These fault zones correspond to N60°E-directed normal faults as shown by seismic profiles and structural studies (Hung & Wiltschko, 1993; Lee *et al*., 1993; Yu & Chou, 2001). In the centre of the basin, a major south-facing fault oriented N60°E, the Yichu Fault (Fig. 3c), separates the Peikang High from the Tainan Basin to the south. Such patterns of sedimentation indicate that the Miocene subsidence was governed to a first order by syn-rift then post-rift extension (i.e., after 30 Ma) in the Chinese margin. In contrast, the Pliocene depocentres (Fig. 8b) are trending ~N10°E, i.e., parallel to the mountain belt, emphasizing the deepening of the basin towards the east in good agreement with the development of the flexural basin. The westwards extent of Pliocene deposits remarkably mimics the shape of the current flexural bulge (Fig. 2). This reveals that most of the Pliocene sediments onlap the forebulge. During the Pleistocene, the depocentre shifts towards the Chinese continental margin. The forelandward migration of the basin depocentre outlines the propagation of the Taiwan foreland basin system including the fold-thrust belt and the peripheral bulge (Fig. 8c).

Results of the subsidence analysis

We distinguish three domains of homogeneous subsidence history in the West Taiwan Basin, which correspond to en-échelon sub-basins in the Chinese margin. From north to south, they are: the Taihsi Basin (Miaoli area), the Taichung Basin (Taichung area) and the Tainan Basin

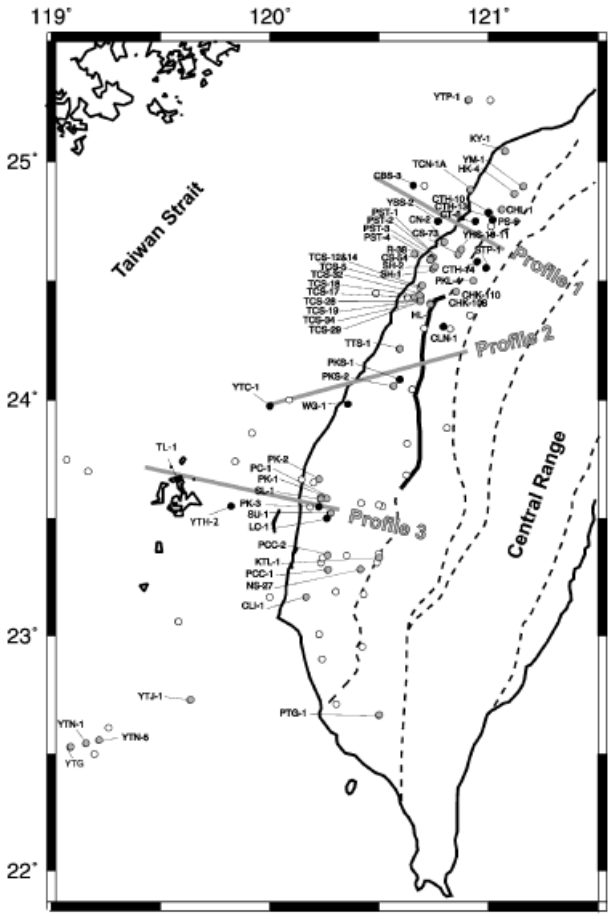

Fig. 7. Location of well data in the western foreland of Taiwan available to this study. Wells in grey are those used in subsidence analysis. Wells shown as black circles were used for the reconstruction of two-dimensional plate deflection evolution. Profile 1 is shown in Fig. 10; Profiles 2 and 3 are used in modelling of Figs 10, 12 and 13. The dashed lines represent the limits of the main tectonic units across the fold-thrust belt. Black heavy shown at the front of the fold-thrust correspond to the active Chelungpu Fault.

(Chiayi and Tainan areas). Figure 9 shows the evolution over time of the decompacted depths and Airy tectonic subsidence for several wells located in the Taihsi, Taichung and Tainan basins. The palaeobathymetry is shown above each diagram. Where possible, we have also performed three serial 50-km-long E-W profiles of well-based tectonic subsidence (Fig. 10). Those profiles illustrate the way the tectonic signal modified the subsidence pattern in the West Taiwan Basin, especially the transition from convex downward to convex upward shape of subsidence profile that outlines the development of a flexural bulge.

The Taihsi Basin (Miaoli area)

The subsidence plots in the Taihsi Basin (Figs 7–9) show three distinct periods, with two main transitions at 14 and 4 Ma. On average, from Oligocene to middle Miocene (top of the Talu Formation: 14.6 Ma), the basin was subsiding rather slowly, indicative of thermal subsidence related to cooling of the thinned Eurasian lithosphere (Lin et al., 2003). The rapid increase of the subsidence at 25–23 Ma corresponds to the post-rift extension episode described by Lin *et al.* (2003). Then, at about 14 Ma, the rate of basin subsidence decreased in wells YSS-2, CT-8, STP-1, YHS-10 and even uplift may be tentatively proposed for some wells such as well PST-1. One further notices a period of quiescence at 12–10 Ma. The possible effect of the palaeobathymetry and compaction of the underlying formations especially of the Talu Formation will be examined below. After this period of quiescence that ceased at *ca*. 4 Ma (i.e., base of the Chinshui Formation), the subsidence rates increased again.

Figure 10 shows E-W profiles of the tectonic subsidence, i.e. without the effect of the sediment load. In the Miaoli area (Taihsi Basin) during the late Oligocene and early Miocene, between ~25 and 17 Ma, the basin subsided slightly faster in the east than in the west (Fig. 10) in agreement with increasing thermal subsidence basinward. For instance, well CBS-3 subsided by ~200 m whereas well STP-1 to the east subsided by ~600 m. At wells CTH-10 and PS-4, between 23 and 20 Ma, a localized uplift (~10 km width) is observed supporting the post-rift extension reported for some parts of the foreland at that time (Lin *et al.*, 2003). During the Early-Middle Miocene, between 17 and 12.5 Ma, a noticeable change occurred. The profile of subsidence changed from convex downward to convex upward. This is illustrated by well CT-8 that recorded less subsidence than the adjacent well CBS-3 and YSS-3. The uplift amounts to ~100 m, which is in the range of most forebulge heights (Crampton & Allen, 1995). Then, in the interval between 5.3 and 4 Ma, we notice that the eastern part recorded more subsidence than the western area that even underwent a relative uplift. This subsidence pattern seems consistent with the development of plate flexure. After 4 Ma, the subsidence increased again by nearly similar amounts in all wells. This illustrates the migration of the basin subsidence forelandward with the advance of thrust units.

The Taichung Basin

The initial subsidence pattern in this area resembles that of the Taihsi Basin (Fig. 9). However, after 14 Ma, the quiescence period recognized northward is clearer and is even associated with uplift in well PKS-1 and WG-1. This uplift is observed between 14.6 and 12.5 Ma, which is the time of the deposition or non-deposition/erosion of the regressive sequence of the Nanchuang Formation. This episode is followed by the deposition of the transgressive sequence of the Kueichulin Formation. This transition probably produces the margin unconformity at the base of the foreland observed in the seismic images of Fig. 3.

Hereafter, we examine the possible effects, that lead to overestimation of the bulge uplift. For instance, more erosion at well WG-1 at that time would have resulted in less subsidence increasing the uplift effect. It is also important to note that the top of the Talu Formation dated at 14.6 Ma indicates a deep bathymetry (Fig. 9). By contrast, both the

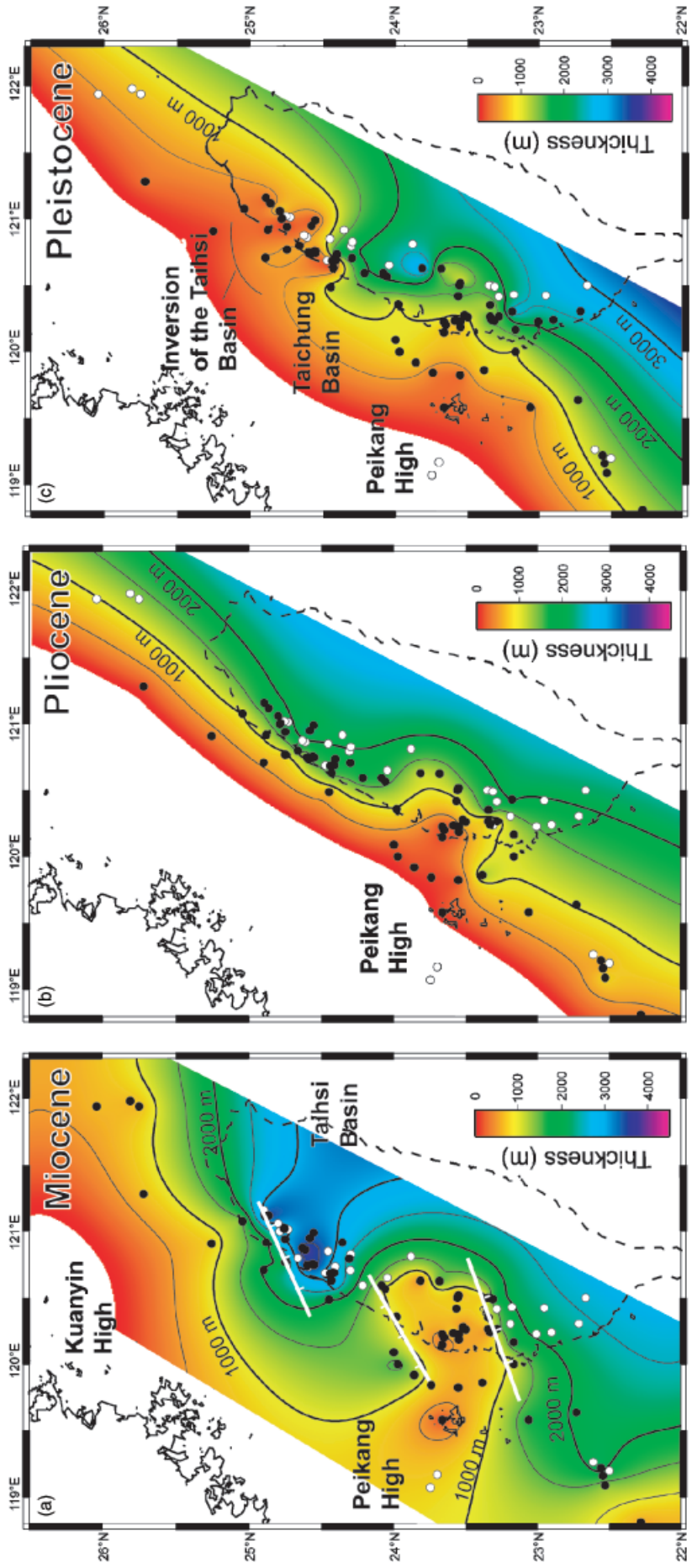

Fig. 8. Isopach maps of the Miocene (a) Pliocene (b) and Pleistocene (c) strata according to the stratigraphic compilation of Fig. 5. The Taihsi Basin that is inherited from the Paleogene extension seems to be active during the Miocene period. Some major extensional faults are probably active at that time such as the Yichu Fault bounding the Peikang High to the south. The Peikang High remains visible until the end of the Pliocene. The orientation of the depocentres suggests that the flexure of the Chinese continental margin clearly controls the West Taiwan basin development during the Pliocene period. The Pleistocene is outlined by the westward propagation of the depocentres, which may be a response of the propagation of the Taiwan orogenic wedge. At the same time, the Taihsi Basin is uplifted and inverted (Huang *et al.*, 1993; Shen *et al.*, 1996; Mouthereau *et al.*, 2002).

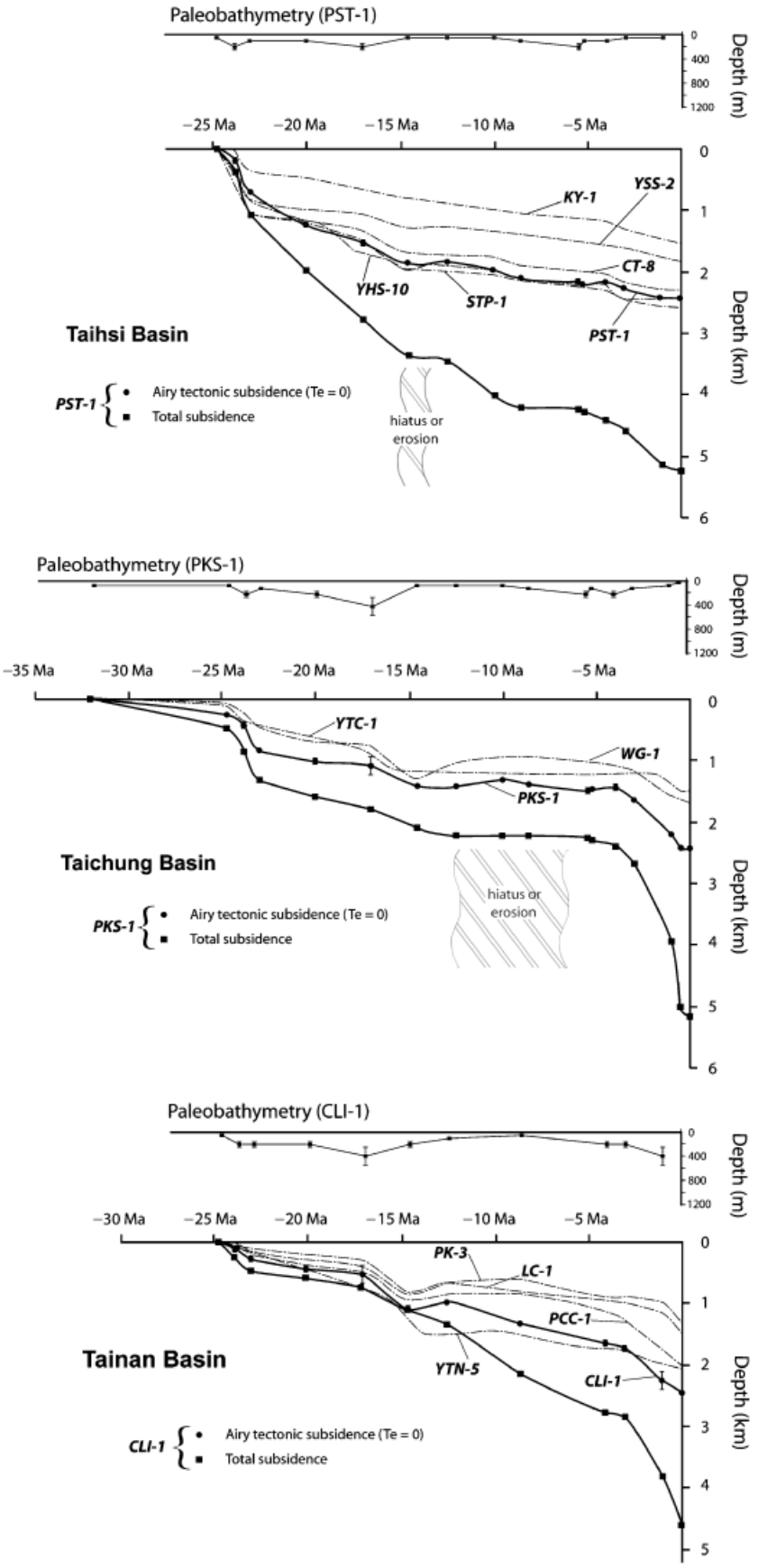

Fig. 9. Subsidence analysis in the Taihsi Basin, Taichung Basin and Tainan Basin. Both tectonic subsidence and decompacted depths over time are shown for PST-1, PKS-1 and CLI-1 wells, which are used as reference wells for Taihsi Basin, Taichung Basin and Tainan Basin, respectively. The palaeobathymetry derived from the study of sedimentary facies is shown above each diagram. Note that the subsidence history is strongly variable along the strike of the Taiwan foreland.

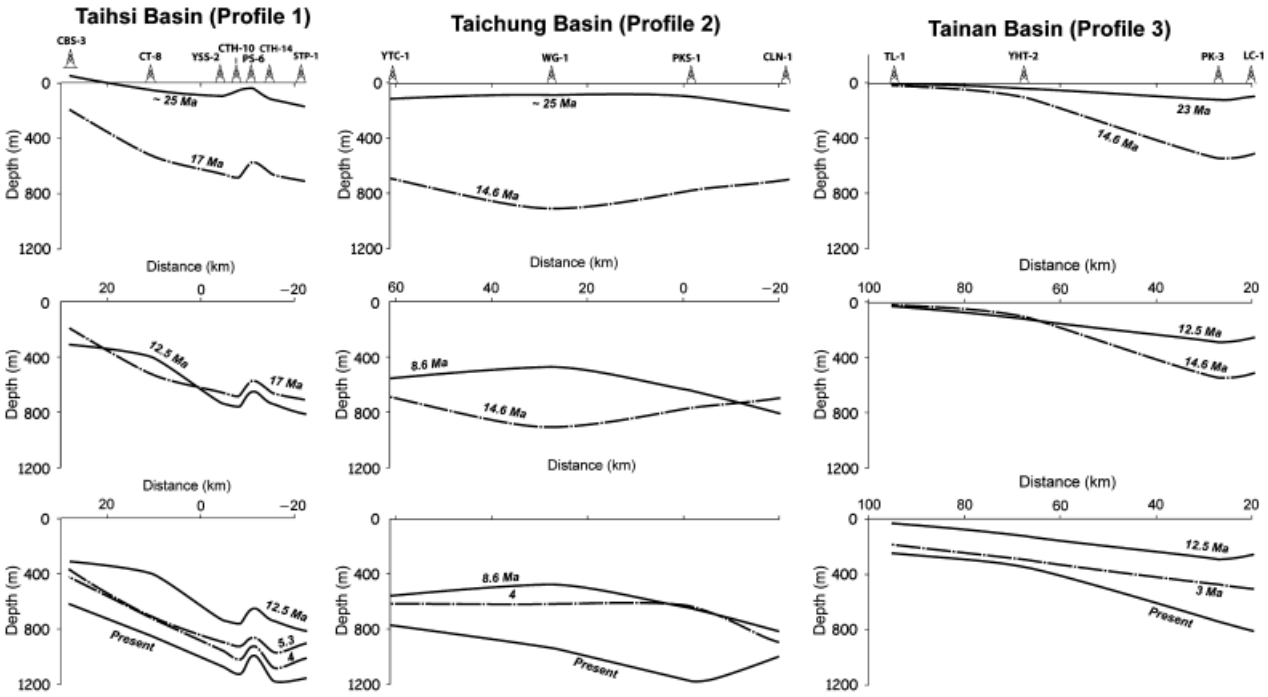

Fig. 10. Profiles of tectonic subsidence in the Miaoli, Taichung and Tainan Basin during the Neogene. Profile number refers to profiles shown in Fig. 7. Note that a significant change occurred after 14.6 Ma. All profiles show a subsidence signal that changed from convex downward to convex upward.

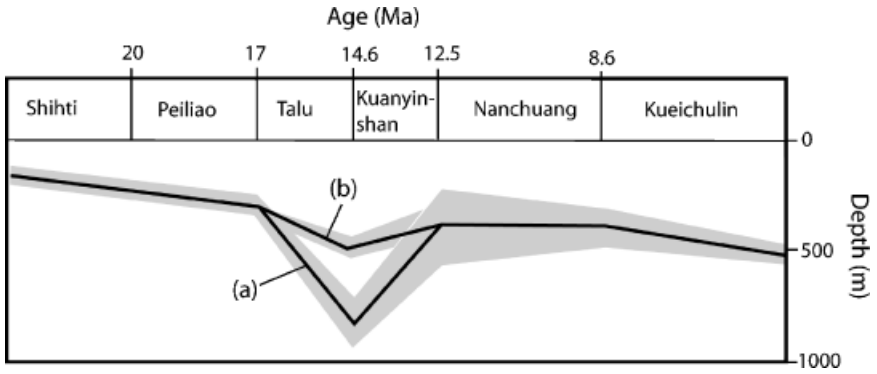

Fig. 11. Estimated effects, on the tectonic subsidence, of both overestimates of the palaeobathmetry of the Talu Formation and erosion. Subsidence obtained in Fig. 9b (a); subsidence in case of overestimate of 300 m (b), results for the same palaeobathymetry error and erosion of 100 m.

palaeobathymetry of the shallow-marine Kueichulin Formation and the erosion of the Kuanyinshan Formation indicate a relatively shallow bathymetry at 12.5 Ma. Even assuming an error of 300 m on the estimate of the palaeobathymetry of the Talu Formation, the uplift is present (Fig. 11). We conclude that despite erosion and uncertainties in the palaeo-water depths of the Talu Formation, the subsidence analysis still predicts uplift. We consequently suggest that a correlation can be made after 14.6 Ma between the period of tectonic quiescence on the Chinese continental margin in the Taihsi Basin and the period of uplift in the Taichung Basin. The second boundary at 4 Ma is followed by a rapid increase of the subsidence during the whole late Pliocene–Pleistocene times.

Along E-W profile 2 (Fig. 10), the subsidence patterns show an initial stage of slow subsidence between 25 and 14.6 Ma, in agreement with observations in the Taihsi Basin. The main stages of the basin development recognized to the north are also identified in the Taichung Basin. The transition from convex downward to convex upward profile is observed with a maximum uplift at well WG-1 on the Peikang High. With respect to the north, the uplift of the continental margin occurred slightly later at 14.6 Ma instead of 15.6 Ma. Since 4 Ma, the maximum subsidence area is shifted to the west. This presumably reflects the migration of the foredeep, in response to the westward propagation of the orogenic loading.

The Tainan Basin

Clear changes at 14 and 4 Ma also divide the subsidence history of the Chiayi area into three stages (Fig. 9). The main difference with respect to the Taichung area lies in the amplitudes of the tectonic movements. First, the subsidence rate between 32 and 14 Ma is about the half that of the Taichung Basin (Fig. 9). The presence of the Peikang basement high (wells PK-3, LC-1 and PCC-1) being less affected by rifting provides an explanation for this pattern of subsidence. However, consistent with previous areas, the uplift occurred between 14.6 and 12.5 Ma (Fig. 10). The uplift essentially affected wells located on the Peikang High such as wells PK-3 and LC-1 uplifted by ~300 m. The subsidence for wells located offshore is little modified at that time. The second change dated at 4 Ma northward, occurred later, at 2 Ma (LC-1 well). The erosion could partly explain this apparent delay. This is consistent with evidence of subaerial gravitational instabilities reported on the northern edge of the Tainan Basin at that time (Chou, 1980; Hong, 1997; Fuh, 2000). After 4 Ma and especially during the Pleistocene, the subsidence rate seems to be more important than elsewhere. Unfortunately, the distribution of well data in this part of the West Taiwan Basin makes interpretations more questionable.

Summarizing, the subsidence patterns in the Taiwan foreland reveal that the Chinese continental margin recorded three major tectonic stages. These episodes are roughly synchronous over the whole West Taiwan Basin and may be tentatively placed in the framework of the geological history of the Taiwan region. We distinguish: (1) a stage of thermal subsidence related to the long-term decay of heat in the mantle associated with the spreading of the South China Sea (~30 to ~14.6 Ma); this stage is interrupted by a post break-up extension at approximately 20 Ma, whose origin has been discussed in previous studies (Lee *et al*., 1993; Lin *et al*., 2003) and is beyond the scope of this paper; (2) a still enigmatic episode of uplift and tectonic quiescence occurred in most areas of the West Taiwan Basin (~14.6 to ~8.6 Ma); and (3) a change of the basin shape together with an increase of the subsidence to the east while the Chinese margin was uplifting (~4 Ma to present).

The episode of uplift at the Middle-Upper Miocene is still a matter of debate. Lin *et al*. (2003) recently interpreted this uplift as being caused by local normal faulting during an episode of post-rift extension, which extended from Middle Miocene from 12.5 to 6.5 Ma. Even though this possibility is supported by the existence of a limited post-rift extension in the Pearl River Mouth Basin at ~14–12 Ma (Clift & Lin, 2001), we rather suggest, based on the subsidence analysis, that this extension might be caused by the passage of the forebulge in the Chinese continental margin. To support this latter possibility, we should notice that the whole basin suffered a tectonic quiescence or uplift over a wide region of ~40–60 km. Furthermore, this episode is associated with erosion, non-deposition or shallowing-upward deposition (Nanchuang Formation) in the whole basin. We suggest that this episode is related to forebulge development, which may be locally amplified by erosion and possibly in association with movements in the hanging wall of reactivated normal faults. We note that the flexure recorded at ~4 Ma occurred coevally throughout the basin. Based on the observations presented above, we infer that the long-term period of static uplift (14.6–4 Ma), followed by a period of migrating uplift (4 Ma-present), results from a unique process in relation with the development of a lithospheric bulge rather than two distinct mechanisms. In order to test this hypothesis, we perform flexure modelling.

MODELLING OF THE FOREBULGE RISE AND MIGRATION

Fitting geometrically the decompacted depths by a deflection profile

Our first concern is to fit geometrically the decompacted depths of the base of the foreland obtained from the subsidence analysis with a universal deflection profile. This study requires (1) the choice of a reference isochronous horizon, belonging to the margin sequences, whose deflection will be modelled and (2) an estimate of the elastic thickness T_e of the continental lithosphere. The position of the plate break is not fixed *a priori* and it is rather a result of the modelling. Only three to four wells contain sufficient stratigraphic records to perform the modelling satisfactorily. As they are aligned along two profiles across the foreland, which is the current width of the foredeep, they are considered to describe the overall development of the basin.

The lithospheric bulge is assumed to be formed after 14.6 Ma (top of the Talu Formation, see Fig. 4) in the Taichung and Tainan basins. For comparison of the development of the plate deflection in both areas, we used the decompacted depth to the 14.6 Ma isochron. Taking advantage of the recent estimates of the effective elastic thickness for the Chinese continental margin (Lin & Watts, 2002; Mouthereau & Petit, 2003) and in order to cover a sufficient range of possible T_e, we calculate flexure profiles for elastic thickness between 10 and 20 km. The deflection profiles obtained are shown in Fig. 12.

From 14.6 to 4 Ma, the plate deflections reconstructed from the decompacted depths depict the increase of the plate curvature to the east of wells PKS-1 and LC-1, as well as the increase of the bulge approximately at wells WG-1 and YTH-2. In detail, the bulge developed mainly between 14.6 and 8.6 Ma. Then until 4 Ma, the height of the bulge decreased with regard to the initial reference level of the Talu Formation.

In the Taichung area, away from the Peikang High, the uplift is observed over 50 km from well WG-1 to PKS-1. Over the Peikang High, the uplifted domain has roughly the same width (Fig. 12). We note that as the bulge developed over the Peikang High, it was eroded (e.g., YTH-1, PK-3

wells), whereas it was buried in the adjacent Taichung Basin. During 10 m year^{-1}, no significant westward translation of the plate deflection was detected. Between 4 and 3 Ma, the plate curvature slightly diminished as the forebulge decreased. After 3 Ma, the Taichung Basin was rapidly subsiding as the load produced by the synorogenic sediments supplied to the basin became important. Coevally, the plate deflection profile migrated towards the foreland.

Numerical modelling of the plate flexure

We suggest that during the mid-Miocene, the Chinese continental margin recorded a flexurally controlled uplift (Figs 8–12). This uplift (or quiescence stage) was initiated coevally along the strike of the foreland basin after 14.6 Ma. We identified an initial static stage during which the bulge was growing vertically without noticeable horizontal foreland-ward migration. It is followed by a stage at 4 Ma, characterized by the acceleration of the subsidence throughout the Taiwan foreland basin. This stage marks the beginning of the westward migration of the forebulge and of the subsiding domain (Fig. 12) into the foreland, in agreement with the progressive onlaps of the Kueichulin Formation (Fig. 2). This second stage is coeval in all parts of the basin except in the Chiayi area where it appeared later (at *ca*. 2 Ma). This bimodal evolution of the plate flexure deserves further attention. We now examine through numerical modelling of the flexure of an elastic broken plate the load history and the bending moments that best fit the data.

Stage 1: Initiation and growth of the flexural bulge (from 14 to 4 Ma)

Hereafter, we attempt to fit the deflection of margin strata corresponding to the Talu Formation with that predicted by numerical modelling. Plate deflections are calculated for T_e of 10 and 20 km and for variable bending moments (Fig. 13). These T_e correspond to extreme bounds of possible values. Recent modelling has derived elastic thicknesses up to 14 km in some parts of the South China shelf (Braitenberg *et al*., 2006), in agreement with T_e of 13 km derived from flexure modelling by Lin & Watts (2002) and slightly higher values of 15–20 km by Mouthereau & Petit (2003) at the latitude of Taiwan. Lower values for T_e (< 5 km) as suggested in the Pearl River Mouth Basin and larger values are not able to fit the data.

In a second time, flexure modelling reveals that subsidence signal can be modelled by the flexure of an elastic plate (T_e between 10 and 20 km) since 12.5 Ma. The bending moment is assumed to represent the cumulative effects of the interaction with another plate (e.g., vertical load, shear stresses at plate boundary, in-plane stresses) and loads acting on the plate (e.g., slab pull, downgoing convective flow).

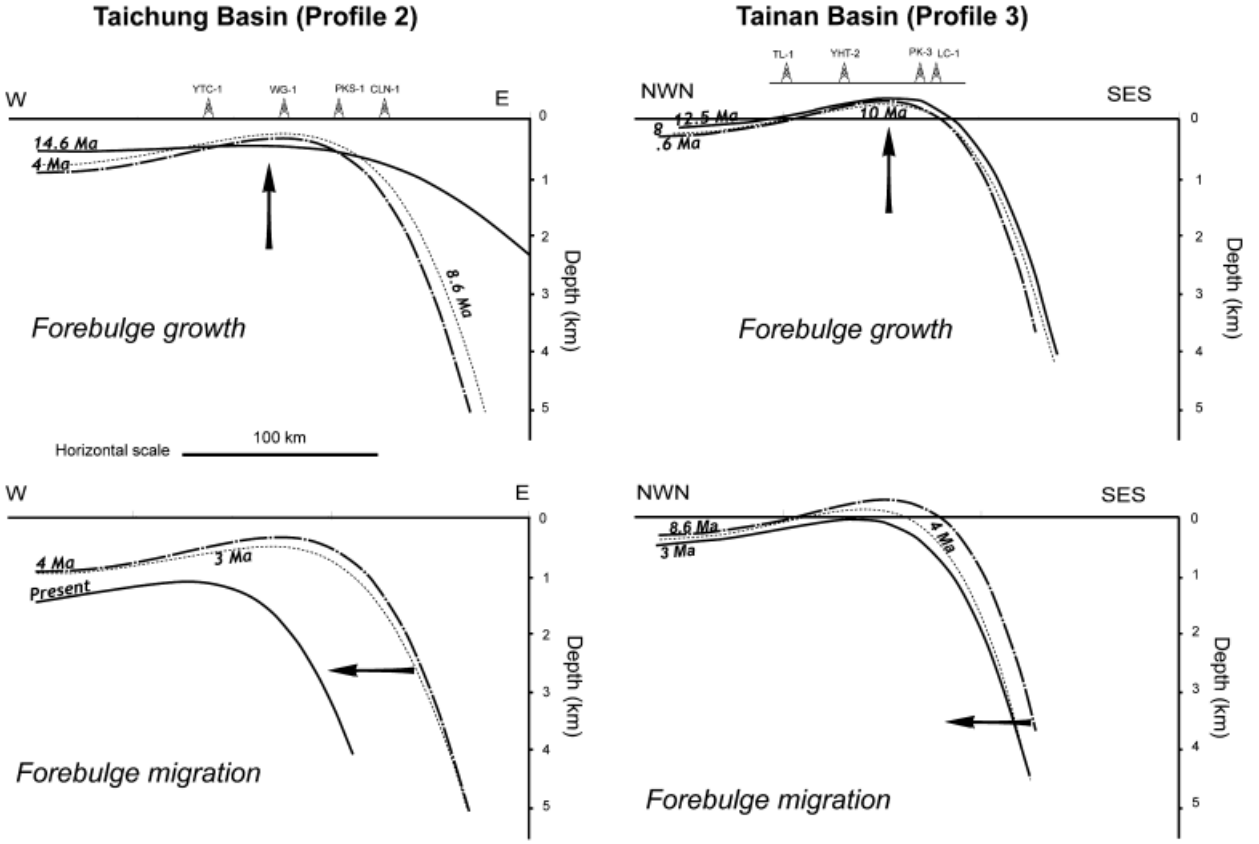

Fig. 12. Geometric modelling (in the sense of the universal deflection profile) of the deflection of the top of the Talu Formation (circles) based on the subsidence analysis. Deflections obtained are shown for Taichung Basin (Profile 2) and Tainan Basin (Profile 3) for an elastic thickness of 10 km only (see text for explanations).

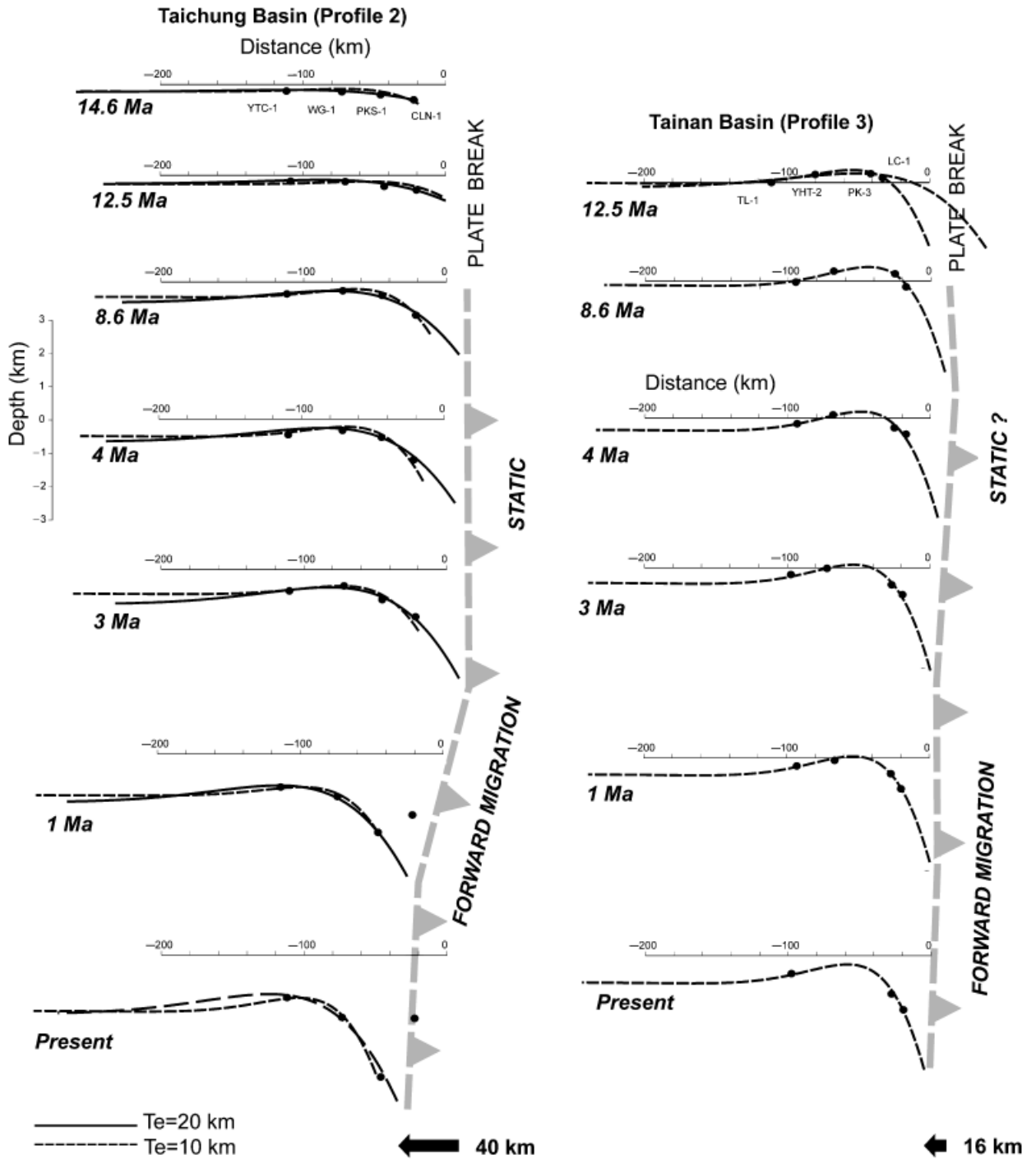

Fig. 13. Numerical modelling of the plate flexure of a purely elastic plate for the Taichung Basin (Profile 2) and Tainan Basin (Profile 3). Parameters such as bulge heights and bending moments at each time step are shown in Table 2 (see text for more explanations).

No surface topography is assumed and moments are applied at the plate end.

We first examine the case of the Taichung Basin (compare with Fig. 12). At 14.6 and 12.5 Ma, the subsidence in the Taichung Basin is limited so the solution for the plate deflection is not really sensitive to the choice of T_e. Moments are also limited with $M \leq 10^{16}\,N\,m\,m^{-1}$ (Table 2). A significant change in the subsidence occurs all over the basin at 12.5 Ma as the top of the Talu Formation is regionally uplifted. However, no bulge can be clearly identified, so the existence of a regional plate flexure cannot be unambiguously confirmed at that time in this part of the foreland. After this point, the behaviour of the plate is dramatically modified. Indeed, at 8.6 Ma the plate curvature increases and a bulge domain can clearly be observed at the location of well WG-1 (Fig. 13). Bending moments also increase up to $1.5–6 \times 10^{16}\,N\,m\,m^{-1}$ (Table 2). The height of the bulge increases by almost 200 m relative to the regional base level of the Talu Formation (Fig. 14). The coeval erosion of the bulge was already observed in

subsidence curves of Fig. 9 and corresponds to the removal of part of the Nanchuang Formation. This erosion is also visible in Fig. 2. We infer that the flexural response of the Eurasian plate to loading occurred between 12.5 and 8.6 Ma. An initial period during which the whole basin seems to be uplifted and migrated eastward is detected. However, uncertainties do not allow us to strengthen this possibility.

In the Tainan Basin, the flexural response of the continental plate to loading remarkably differs in time and space. The best fit is always obtained for lower T_e, which is in good agreement with T_e estimates from gravity modelling (Mouthereau & Petit, 2003). As early as 12.5 Ma, a tectonically induced uplift is clearly observed at the location of well PK-3. The bulge height is more important, ~400 m, more than northward (Fig. 13), which is consistent with relatively higher moments of 3.5×10^{16} N m m^{-1}. The good fit with the theoretical deflection suggests that it is of flexural origin. The bulge then increases at 8.6 Ma to reach more than 500 m (Fig. 14). The margin sequences are uplifted above sea level and part of the Nanchuang Formation is eroded away from the bulge. By contrast with the Taichung Basin, the bulge is dominantly subaerial and eroded. The higher plate curvature is correlated with significant moments of 2.5–7 $\times 10^{16}$ N m m^{-1} and a weaker plate.

Table 2. Results of flexure modelling shown in Fig. 13

	Taichung Basin (Profile 2)		Tainan Basin (Profile 3)	
Ma	M (10^{16} Nm m^{-1})	z_b (m)	M (10^{16} Nm m^{-1})	z_b (m)
14.8	0.5–1	78–55		
12.5	0.5–1.5	78–83	2.5–7	391–387
8.6	1.5–6	234–332	3.5–?	547
4	1.8–7	281–387	3.5–?	547
3	1.5–8.5	234–470	3.5–?	547
1	1.5–8.5	234–470	3.5–?	547
0	2.5–10	391–553	3.5–?	547

Bending moments (M) and forebulge heights (z_b) are shown for both studied profiles 2 and 3 and for different time steps. Both values of the bending moments and bulge heights correspond to T_e of 10 km and 20 km on the left and on the right, respectively.

Stage 2: Forelandward migration and burial of the forebulge (from 4 Ma to present)

After 4 Ma, both the activity of thrust faults (Fig. 15) and the increase of sediment accumulation on the margin (Fig. 16) suggest that the surface topography related to the growth of the Taiwan orogen became important. Until 3 Ma, the position of the bulge and the position of the applied load are unchanged (Fig. 13); the basin width is also consequently unchanged. In parallel, the bending moments increased and the forebulge height increased (Figs 13 and 14). After 3 Ma, in the Taichung Basin, and 8.6 Ma, in the Tainan Basin (Profile 3), the basin has migrated forelandward by about 40 and 16 km, respectively. We note that no changes in the bending moments are required in the Tainan Basin (Profile 3) so the forebulge height remains constant. In contrast, an increase of bending moments is necessary to fit the data in the Taichung Basin. The shift of the plate break after 3 Ma (Taichung Basin) remarkably coincides with the involvement of the site of well CLN-1 into deformation, as it is suggested by the anomalous

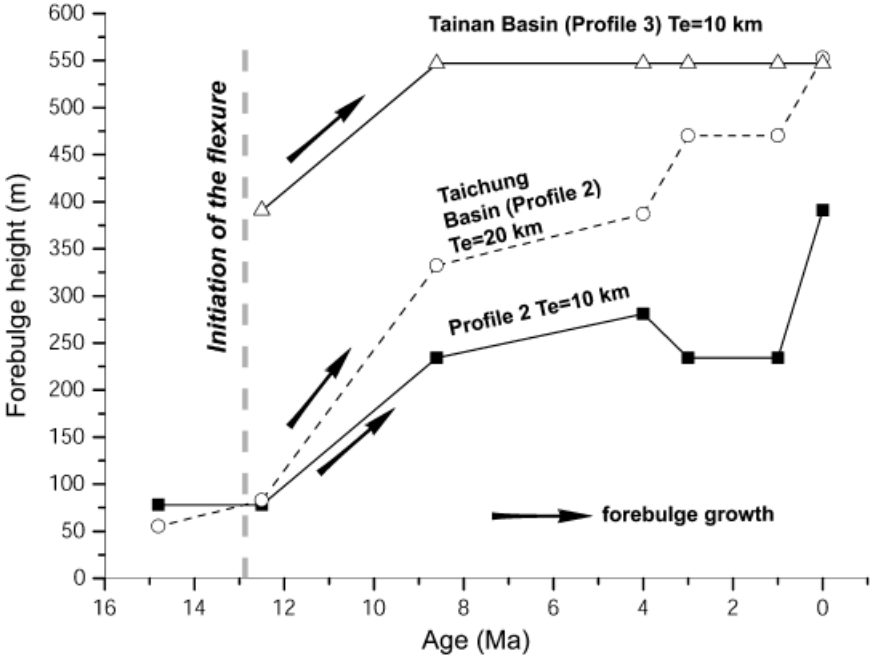

Fig. 14. Evolution of the forebulge heights relative to a regional reference level defined by the top of the Talu Formation in the Tainan Basin (Profile 3) and the Taichung Basin (Profile 2). The rapid increase in forebulge uplift reveals the onset of the plate flexure at 12.5 Ma. The systematically higher height of the bulge on the edge of the Tainan Basin (Profile 3) reveals the presence of a weaker lithosphere.

uplift of the Talu Formation that could not fit plate deflection. Taking into account the location of well CLN-1 (Fig. 7), we suggest that the uplift is caused by reverse movement in the hangingwall of the currently active Chelungpu fault. Hence, the eastern part of the foredeep became a part of the fold-thrust belt after 3 Ma.

We note that the contributions of the sediment loading to the deepening of the basin were significant throughout the history of the foreland basin. Since 3 Ma, the accumulation of synorogenic sediments (Fig. 16) induced the burial of the plate. An example is provided by well PKS-1 of the Taichung Basin for which the contribution of sediment loading to subsidence reaches about 50% in the past 1 m year^{-1}. (see Fig. 9). As outlined by the study of fission-track dating (Liu, 1982) and sedimentation accumulation in the foreland (Fig. 16), the rates of the sediment supply into the basin significantly increased after 2 Ma in response to the fast exhumation and bedrock-controlled erosion of the hinterland. In the context of large volumes of sediments supplied to the basin and changes in the shape of the orogenic wedge, we expect a removal of the forebulge or at least a decrease in the vertical growth of the bulge in response to the spreading of sedimentary loading in the foreland. In contrast, the bulge continues to grow over time (Fig. 13). This suggests that the applied moments increased sufficiently through time to balance the sedimentary loading onto the flexural bulge. Moreover, the dispersal of the sediments within the foreland basin towards the South China Sea after 2 Ma (see Fig. 13) may have been efficient enough to limit the sedimentary loads. This is supported today by the lack of large alluvial fans at the thrust front despite the high sediment accumulation. The Peikang promontory (Chiayi area) was not buried beneath the synorogenic sediments before 1 Ma. Remarkably, the deflection profile has been little modified since 8.5 Ma until today. The geographic position of the bulge also remained nearly unchanged over the Peikang promontory.

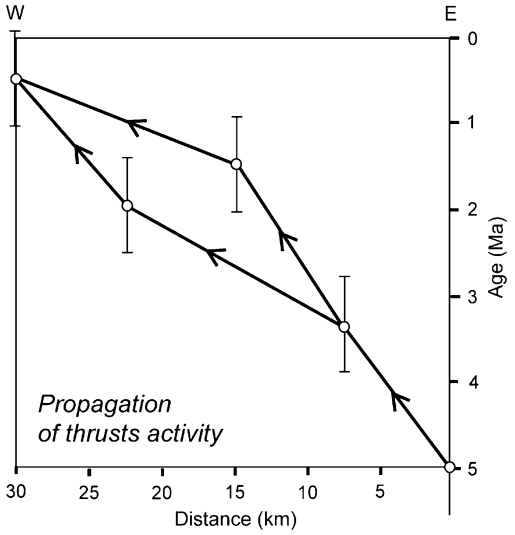

Fig. 15. Age of the thrusts' initiation in the southern Western Foothills scheme based on tectonic–sedimentation relationships after Mouthereau *et al.* (2001). This figure shows that an abrupt increase in the thrust activity occurred after 3–4 Ma. The thrust front moved at a rate of about 6–7 km m year^{-1}, since 3 m year^{-1}. For comparison, the flexure migrated at about 2 km m year^{-1}, since 8.5 m year^{-1}, in the Tainan Basin and at 13 km m year^{-1}, since 3 m year^{-1}, in the Taichung Basin.

DISCUSSION AND CONCLUSIONS

Plate flexure at the irregular Chinese continental margin and origin of extension in the Middle-Upper Miocene

We have noticed that differential accommodation of the plate flexure occurred between the Taichung Basin and the Peikang promontory (Fig. 17). For instance, the strata

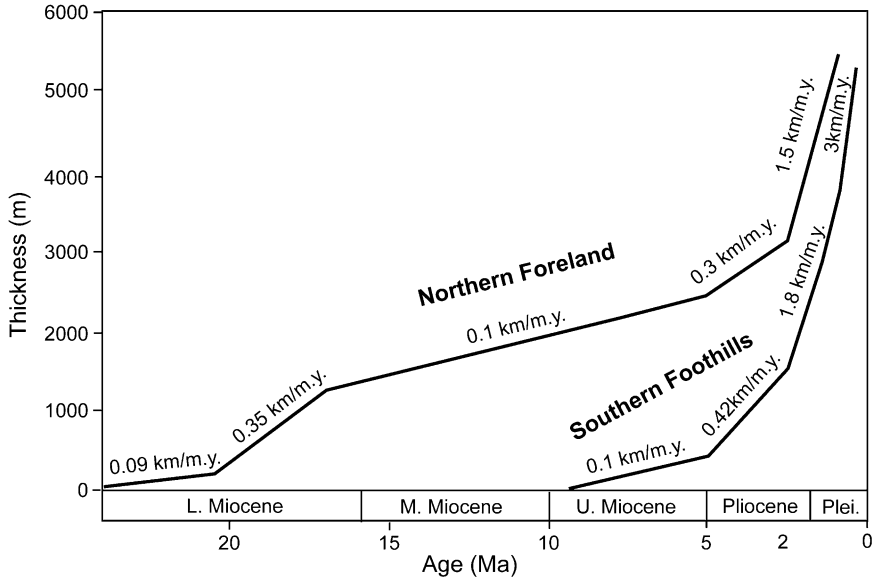

Fig. 16. Sediment accumulation in the Taiwan foreland after Chang & Chi (1983).

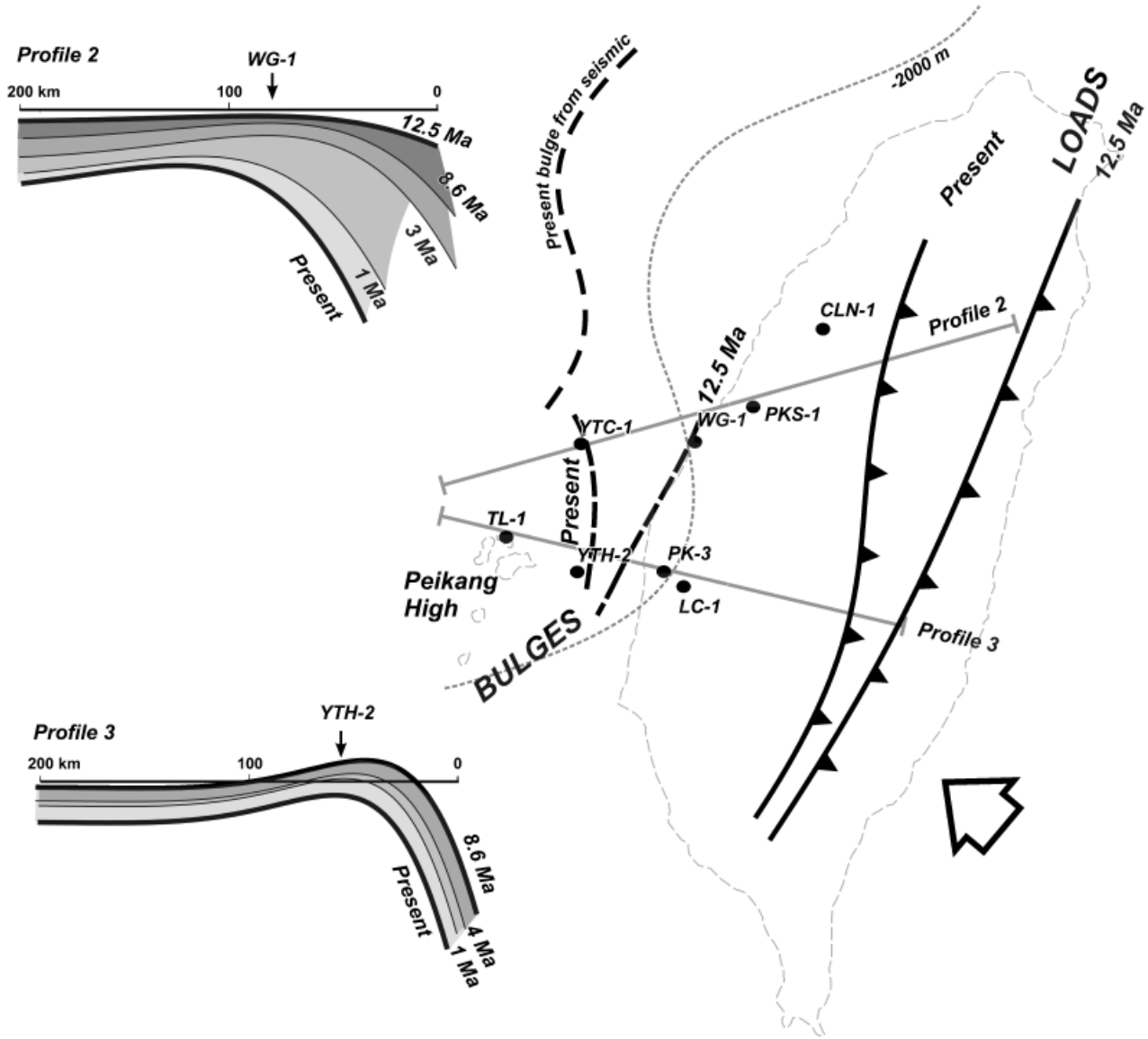

Fig. 17. Position of loads and bulges, in the Taiwan region, reconstructed from numerical modelling at different time steps (Fig. 12). The forelandward propagation of the foreland basin system is clearly more pronounced at the latitude of the Taichung basin. The positions of the plate break are extrapolated towards the North and the South with regard to the E-W profile extents (in grey).

of the Nanchuang Formation were more uplifted and eroded on the Peikang High than in the adjacent continental re-entrant of the Taichung Basin. The differential amounts of vertical uplift and erosion at the Peikang High are an illustration of the distribution of the long-term mechanical weakness of the Eurasian plate along strike. This has already been suggested from current plate flexure based on gravity data modelling (Mouthereau & Petit, 2003). Other geophysical evidence of this mechanical weakness is provided by the extensional focal mechanisms observed along the Yichu Fault (Lin & Watts, 2002) and Plio–Pleistocene normal faulting (Figs 2 and 3). We suggest that a flexurally controlled extension has reactivated some of the inherited Palaeogene normal faults of the Chinese continental margin, especially where pre-orogenic extensional basins exist, e.g. in the Tainan Basin, south of the Peikang High. The passage of the forebulge at 12.5 Ma into an inherited weaker portion of the Chinese margin would have produced an increase in plate curvature and renewed extension, leading to enhancement of the bulge uplift and its localization for a prolonged period of time. This mode of extension is confirmed by the current plate deflection that reveals high curvature $\sim 1.2 \times 10^{-6}\,\mathrm{m}^{-1}$ and predicts extension in the whole upper crust down to 10 km (Mouthereau & Petit, 2003). This is a possible illustration of the effect of inelastic yielding of the inherited weaker portion of the lithosphere that could localize uplift for long time periods ($\sim$5–6 m year^{-1}) in the foreland (Waschbush & Royden, 1992). In this interpretation, the extension observed in the Middle-Upper Miocene is related to flexure in a compressional setting, not to a rifting event.

Flexure modelling further suggests that the Peikang promontory was subaerially exposed earlier on the north-

ern edge of the Tainan Basin (Profile 3) than to the edge of the Taichung Basin (Profile 2). To the first order, this is probably a consequence of the inherited topography of the Peikang promontory. The obliquity of the Chinese continental margin with respect to the plate convergence and thus to the migration of the orogenic wedge may also provide an additional explanation. The plate convergence is nearly normal to the southern edge of the Peikang promontory, whereas it is slightly oblique to the North in the Taichung Basin. This is shown by strongly variable structural styles at the front of the fold-thrust belt (e.g. Mouthereau *et al*., 2002). As a consequence, at a given time, the load resolved to the South of the Peikang High should be higher than the load necessary to flex the plate at the latitude of the Taichung Basin. Changes in the load probably reflect the increase of the orogenic loading and/or the buildup of stresses due to the variations in plate interactions. We conclude that in addition to the presence of inherited weaker parts of the lithosphere and mechanical yielding, the shape of the continental margin may have influenced the development of the forebulge and the flexural deflection in the West Taiwan Basin.

What controlled the plate flexure in the Middle-Miocene?

Flexure modelling indicates that the Eurasian lithosphere was possibly flexed since 12.5 Ma in response to loading applied in the east of Taiwan (Fig. 17) close to the current position of plate suture, i.e., at the Longitudinal Valley Fault (Figs 1 and 2). The onset of plate flexure is coeval with the initiation of forebulge uplift, erosion of the Nanchuang Formation, in association with extension in the Chinese margin, and it is followed by the deposition of the transgressive sequence above the bulge unconformity.

In the attempts to place our results in the framework of the geodynamic setting of the Philippines Sea Plate/Eurasia convergence, we must address the origin of the load at 12.5 Ma. We have indicated earlier that the age of the collision and the nature of the collided margin are a long-lived debate. An age of 12.5 Ma for the onset of the arc-continent collision is problematic with regard to most existing plate reconstructions (e.g., Hall, 2002; Sibuet et al., 2004). Indeed, if we consider even very conservative estimates of the plate convergence, e.g., $\sim$56 km m year^{-1} and an age of 9 Ma for the initiation of the arc-continent collision (Sibuet & Hsu, 2004), by backtracking the Luzon arc from its present position, it is still located $\sim$500 km to the east of the point where we locate the applied load at 12.5 Ma. This problem remains if we assume that the collision started later at 6.5 Ma as suggested by Lin *et al*. (2003). The Luzon Arc is still located more than 300 km farther to the Southeast. So placing the beginning of the collision at 6.5 Ma to explain the flexure does not solve the question on the origin of the load. We infer that the only alternative solution is to consider that the load producing the observed plate deflection might not be related to the arc-continent collision.

The Middle Miocene period is characterized by the cessation of the spreading in the South China Sea at $\sim$16 Ma. Local and minor post-rift extension at 14–12 Ma seems to continue due to the very low rigidity of the Chinese margin beneath the Pearl River Mouth Basin as indicated (Clift & Lin, 2001). By 15 Ma, the Palawan-Mindoro continental block that represents the eastern conjugate margin of the Chinese margin is thrusted by the Luzon arc (Hall, 2002). It is at the same time, *ca*. $\sim$15 Ma, that the Manila Trench became active and extended northwards to the Ryukyu subduction zone (Sibuet et al., 2004). The Philippines Sea Plate/Eurasia motion also changed from NNW-SSE-directed to NW-SE-directed (Seno & Maruyama, 1984).

Thus, the Middle-Miocene appears to be a period of dominant compressional setting in the Taiwan area, the Eurasian plate being subducted beneath the Philippines Sea Plate. In this framework, we should mention the presence of ophiolitic blocks known for years in Taiwan and forming part of the Lichi and Kenting melanges. In the Kenting melange, the ophiolitic complex is composed of Oligo-Miocene ultrabasic rocks, pelitic sediments and pillows whose origin probably lies along a transform fault of the South China Sea (Pelletier & Stephan, 1986). An age of Middle-Upper Miocene $\sim$13–14 Ma (NN 6) is suggested for the emplacement of the ophiolites. Because the ophiolitic materials are found within the siliciclastic series belonging to the Chinese margin, Pelletier & Stephan (1986) proposed an obduction of part of the South China Sea during the Miocene. We conclude that the Middle Miocene obduction is a viable alternative to explain the deflection of the Chinese and forebulge initiation in the Chinese margin.

We propose that following the initiation of the plate flexure at 12.5 Ma induced by obduction of part of the South China Sea, loading increased through time (Table 2) but without significant propagation forelandward (Figs 13 and 17). As a consequence, the plate curvature increased, which led to mechanical yielding of the plate producing extension in the upper crust. It was not before 3 Ma that the plate break propagated forelandward, in association with the migration of the Taiwan fold-thrust belt.

ACKNOWLEDGEMENTS

This work was supported by the French-Taiwan cooperation programme. The authors are especially indebted to Andrew T. Lin, Bernard J. Coakley, the Editor Hugh Sinclair and anonymous reviewers for their thoughtful suggestions, which led to improvements in an earlier version of the manuscript.

REFERENCES

Allen, P.A. & Allen, J.R. (2005) *Basin Analysis, Principles and Applications*. Blackwell publishing, Oxford, 549pp.

Angevine, C.L., Heller, P.L. & Paola, C. (1990) Quantitative Sedimentary Basin Modeling. American Association of Petroleum Geologists Shortcourse (Note Series 32): 247..

Barrier, E. & Angelier, J. (1986) Active collision in Eastern Taiwan: the coastal range. *Mem. Geol. Soc. China*, **7**, 135–159.

Berggren, W.A., Kent, D.V., Swisher, C.C. & Aubry, M.P. (1995) A revised cenozoic geochronology and chronostratigraphy. In: *Geochronology, Time Scales and Global Stratigraphic Correlation* (Ed. by W.A. Berggren, D.V. Kent, M.P. Aubry & J. Hardenbol), *SEPM Spec. Publ.* **54** (pp. 129–212.

Bond, G.C. & Kominz, M.A. (1984) Construction of tectonic subsidence curves for the early Paleozoic miogeocline, southern Canadian Rocky Mountains: implications for subsidence mechanisms, age of breakup, and crustal thinning. *Geol. Soc. Am. Bull.*, **95**, 155–173.

Braitenberg, C., Wienecke, S. & Wang, Y. (2006) Basement structures from satellite-derived gravity field: South China Sea ridge. *J. Geophys. Res.*, **111**, B05407 (doi:10.1029/2005JB003938).

Briais, A., Patriat, P. & Tapponnier, P. (1993) Updated interpretation of magnetic anomalies and seafloor spreading stages in the South China Sea: implication for the tertiary tectonics of Southeast Asia. *J. Geophys. Res.*, **98**, 6299–328.

Chang, L.S. (1975) Biostratigraphy of Taiwan. *Geol. Paleontol. SE Asia*, **15**, 337–361.

Chang, S.S.L. & Chi, W.-R. (1983) Neogene nanoplankton biostratigraphy in Taiwan and the tectonic implications. *Pet. Geol. Taiwan*, **19**, 93–147.

Chen, W.-S., Ridgway, K.D., Horng, C.-S., Chen, Y.-G., Shea, K.-S. & Yeh, M.-G. (2001) Stratigraphic architecture, magnetostratigraphy, and incised-valley systems of the Pliocene–Pleistocene collisional marine foreland basin of Taiwan. *Geol. Soc. Am. Bull.*, **113**(10), 1249–1271.

Chi, W.-R. (1978) The Late Neogene Nanobiostratigraphy in the Tainan Foothills Region, Southern Taiwan. *Pet. Geol. Taiwan*, **15**, 89–125.

Chinese Petroleum Corporation (1982) *Geological Map of Taiwan*. Chinese Petroleum Corporation, Miaoli, Taichung, Chiayi, Tainan.

Chou, J.-T. (1971) A sedimentologic and paleogeographic study of the neogene formations in the Taichung region, Western Taiwan. *Pet. Geol. Taiwan*, **9**, 43–66.

Chou, J.-T. (1976) A sedimentologic and paleogeographic study of the Miocene Shihti formation in Western Taiwan. *Pet. Geol. Taiwan*, **13**, 119–138.

Chou, J.-T. (1980) Stratigraphy and sedimentology of the Miocene in Western Taiwan. *Pet. Geol. Taiwan*, **17**, 33–52.

Clift, P. & Lin, J. (2001) Preferential mantle lithospheric extension under the South China Margin. *Marine Pet. Geol.*, **18**, 929–945.

Clift, P.D., Lin, J. & ODP Leg 184 Scientific Party (2001) Patterns of extension and magmatism along the continent-ocean boundary, south China margin, in non-volcanic rifting of continental margins: a comparison of evidence from land and sea. In: (Ed. By R.C.L. Wilson, M.-O. Beslier, R.B. Whitmarsh, N. Froitzheim & B. Taylor), *Spec. Publ. Geol. Soc. London*, **187**, 489–510.

Coakley, B.J. & Watts, A.B. (1991) Tectonic controls on the development of unconformities: the North Slope, Alaska. *Tectonics*, **10**, 101–130.

Covey, M. (1986) The evolution of foreland basins to steady state: evidence from the western Taiwan foreland basin. *Spec. Publ. Int. Assoc. Sedimentol.*, **8**, 77–90.

Crampton, S.L. & Allen, P.A. (1995) Recognition of forebulge unconformities associated with early stage foreland basin development: example from the North Alpin Foreland Basin. *Am. Assoc. Pet. Geol. Bull.*, **79**(10), 1495–1514.

DeCelles, P.G. & Giles, K.A (1996) Foreland basins systems. *Basin Res.*, **8**, 105–123.

Delcaillau, B., Déramond, J., Souquet, P., Angelier, J., Chu, H.-T., Lee, J.-C., Lee, T.-Q., Lee, J.-F., Liew, P.-M. & Lin, T.-S. (1994) Enregistrement tectono-sédimentaire de deux collisions dans l'avant-pays nord-occidental de la chaîne de Taiwan. *C. R. Acad. Sci. Paris*, **318**(II), 985–991.

Flemings, P.B. & Jordan, T.E. (1989) A synthetic stratigraphic model of foreland basin development. *J. Geophys. Res.*, **94**, 3851–3866.

Fuh, S.C. (2000) Magnitude of Cenozoïque erosion from mean sonic Transit time, offshore Taiwan. *Marine Pet. Geol.*, **17**, 1011–1028.

Hall, R. (2002) Cenozoic geological and plate tectonic evolution of SE Asia and the SW Pacific: computer-based reconstructions, model and animations. *J. Asian Earth Sci.*, **20**, 353–432.

Haq, B.U., Hardenbol, J. & Vail, P.R. (1987) Chronology of fluctuating sea-levels since the Triassic. *Science*, **235**, 1156–1167.

Ho, C.-S. (1986) A synthesis of the geologic evolution of Taiwan. *Tectonophysics*, **125**, 1–16.

Ho, C.-S. (1988) An introduction to the geology of Taiwan: explanatory text of the geologic map of Taiwan. Ministry of Economic Affairs, ROC, 192pp.

Holloway, N.H. (1982) North Palawan Block, Philippines: its relations to Asian Mainland and role in evolution of South China. *Am. Assoc. Pet. Geol. Bull.*, **66**, 1355–1383.

Hong, E. (1997) Evolution of Pliocene to Pleistocene sedimentary environments in an Arc-Continent collision zone: evidence from the analyses of Lithofacies and Ichnofacies in the Southwestern Foothills of Taiwan. *J. Southeast Asian Earth Sci.*, **15**, 381–392.

Huang, T. (1968) Some Planktonic Foraminifera from Well Pk-3 at Peikang, Yunlin, Taiwan. *Proc. Geol. Soc. China*, 34–44.

Huang, T.C. (1976) Neogene calcareous nanoplankton biostratigraphy used from the Chuhuang-Keng Section, North Western Taiwan. *Proc. Geol. Soc. China*, 7–24.

Huang, T.C. (1984) Planktonic foraminiferal biostratigraphy and datum planes in the neogene sedimentary sequence in Taiwan. *Palaeogeogr. Palaeoclimatol. Palaeoecol.*, **46**, 97–106.

Huang, T.Y. (1978) Foraminifer biostratigraphy of the Huantzu Section, Southern Taiwan. *Pet. Geol. Taiwan*, **15**, 35–48.

Huang, C.-Y., Wu, W.Y., Chang, C.-P., Tsao, S., Yuan, P.B., Lin, C.W. & Kuan-Yuan, X. (1997) Tectonic evolution of accretionary in the Arc-continent collision terrane of Taiwan. *Tectonophysics*, **281**, 31–51.

Huang, S.T., Chen, R.C. & Chi, W.R. (1993) Inversion tectonics and evolution of the Northern Taihsi Basin, Taiwan. *Pet. Geol. Taiwan*, **28**, 15–46.

Hung, J.-H. & Wiltschko, D.V. (1993) Structure and kinematics of arcuate thrust faults in the Miaoli-Cholan area of Western Taiwan. *Pet. Geol. Taiwan*, **28**, 59–96.

Hung, J.-H., Wiltschko, D.V., Lin, H.-C., Hickman, J.B., Fang, P. & Bock, Y. (1999) Structure and motion of the Southwestern Taiwan fold and thrust belt. *Terres. Atmos. Oceanic Sci.*, **10**(3), 543–568.

Jacobi, R.D. (1981) Peripheral bulge – a causal mechanism for the Lower/Middle Ordovician disconformity along the Western margin of the Northern Appalachians. *Earth Planet. Sci. Lett.*, **56**, 245–251.

Jordan, T.E. (1995) Retroarc foreland and related basins. In: *Tectonics of Sedimentary Basins* (Ed. by C.J. Busby & R.V. Ingersoll), pp. 331–362. Blakwell, Cambridge, MA.

Lallemand, S., Font, Y., Bijwaard, H. & Kao, H. (2001) New insights on 3-D plates interaction near Taiwan from tomography and tectonic implications. *Tectonophysics*, **335**, 229–253.

Lee, J.-C. (1994) Structure et deformation Active d'un Orogene: Taiwan. M.Sc. Thesis, Université Pierre et Marie Curie, Paris, 281pp.

Lee, J.-C., Angelier, J. & Chu, H.-T. (1997) Polyphase history and kinematics of a complex major fault zone in the Northern Taiwan mountain belt: the Lishan fault. *Tectonophysics*, **274**, 97–115.

Lee, T.-Y., Tang, C.-H., Ting, J.-S. & Hsu, Y.-Y. (1993) Sequence stratigraphy of the Tainan basin, offshore Southwestern Taiwan. *Pet. Geol. Taiwan*, **28**, 119–158.

Lin, A.T. & Watts, A.B. (2002) Origin of the West Taiwan basin by orogenic loading and flexure of the rifted continental margin. *J. Geophys. Res.*, **107**(B9), doi: 10.1029/2001JB000669.

Lin, A.T., Watts, A.B. & Hesselbo, S.P. (2003) Cenozoic stratigraphy and subsidence history of the South China Sea margin in the Taiwan region. *Basin Res.*, **15**, 453–478.

Liu, T.-K. (1982) Tectonic implications of fission-track ages from the central range, Taiwan. *Proc. Geol. Soc. China*, **25**, 22–37.

Lorenzo, J., O'Brien, G.W., Stewart, J. & Tandon, K. (1998) Inelastic yielding and forebulge shape across a modern foreland basin: North West shelf of Australia, Timor sea. *Geophys. Res. Lett.*, **25**, 1455–1458.

Lu, C.-Y. & Hsü, K.J. (1992) Tectonic evolution of the Taiwan mountain belt. *Pet. Geol. Taiwan*, **27**, 21–46.

Malavieille, J., Lallemand, S., Dominguez, S., Deschamps, A., Lu, C.-Y., Liu, C.-S., Schnürle, P. & Crew, A.S. (2002) Arc-continent collision in Taiwan: new marine observations and tectonic evolution. In: *Geology and Geophysics of an Arc-Continent Collision, Taiwan, Republic of China* (Ed. by T.B. Byrne & C.-S. Liu), pp. 187–211. Geological Society of America Special Paper, GSA, Boulder, CO.

Mouthereau, F., Deffontaines, B., Lacombe, O. & Angelier, J. (2002) Variations along the strike of the Taiwan thrust belt: basement control on structural style, wedge geometry and kinematics. In: *Geology and Geophysics of an Arc-Continent Collision, Taiwan, Republic of China* (Ed. by T.B. Byrne & C.-S. Liu), pp. 35–58. Geological Society of America Special Paper, GSA, Boulder, CO.

Mouthereau, F., Lacombe, O., Deffontaines, B., Angelier, J. & Brusset, S. (2001) Deformation history of the southwestern Taiwan foreland thrust belt: insights from tectono-sedimentary analyses and balanced cross-sections. *Tectonophysics*, **333**, 293–322.

Mouthereau, F. & Petit, C. (2003) Rheology and strength of the Eurasian continental lithosphere in the foreland of the Taiwan collision belt: constraints from seismicity, flexure and structural styles. *J. Geophys. Res.*, **108**(B11), 2512, doi:10.1029/2002JB002098.

Namson, J. (1984) Structure of the Western Foothills Belt, Miaoli-Hsinchu area, Taiwan: (III) northern part. *Pet. Geol. Taiwan*, **20**, 35–52.

Oinomikado, T. (1955) Micropalaeontological Investigation of the Chishan Standard Section, near Tainan, Taiwan, China. Chinese Petroleum Company Palaeontology Laboratory Report, pp. 7–10.

Pelletier, B. & Stephan, J.-F. (1986) Middle Miocene obduction and Late Miocene beginning of collision registered in the Hengchun Peninsula: geodynamic implications for the evolution of Taiwan. *Tectonophysics*, **125**(1-3), 133–160.

Quinlan, G.M. & Beaumont, C. (1984) Appalachian thrusting, lithospheric flexure, and the Paleozoic stratigraphy of the eastern interior of North America. *Can. J. Earth Sci.*, **21**, 973–996.

Schmidt, V. & McDonald, D.A. (1979) The role of secondary porosity in the course of sandstone diagenesis. *Soc. Econ. Palaeontol. Mineral. Spec. Publ.*, **26**, 175–208.

Seno, R. & Maruyama, S. (1984) Paleogeographic reconstruction and origin of the Philippine Sea. *Tectonophysics*, **102**, 53–84.

Seno, T., Stein, S. & Gripp, A.E. (1993) A model for the motion of the Philippine Sea Plate consistent with NUVEL-1 and geological data. *J. Geophys. Res.*, **98**, 17941–17948.

Sheffels, B. & McNutt, M. (1986) Role of subsurface loads and regional compensation in the isostatic balance of the transverse ranges, California: evidence for intracontinental subduction. *J. Geophys. Res.*, **91**(B6), 6419–6431.

Shen, H.C., Huang, S.T., Tang, C.H. & Hsu, Y.-Y. (1996) Geometrical characteristics of structural inversion on the offshore of Miaoli, Taiwan. *Pet. Geol. Taiwan*, **30**, 79–110.

Sibuet, J.-C. & Hsu, S.-K. (2004) How was Taiwan created? *Tectonophysics*, **379**, 159–181.

Sibuet, J.-C., Hsu, S.-K. & Debayle, E. (2004) Geodynamic context of the Taiwan orogen. In: *Continent-Ocean Interactions within East Asian Marginal Seas* (Ed. by P. Clift, W. Kuhnt, P. Wang & D.E. Hayes), pp. 127–158. AGU, Washington, DC.

Sinclair, H.D. (1997) Tectonostratigraphic model for underfilled peripheral basins: an Alpine perspective. *Geol. Soc. Am. Bull.*, **109**(3), 324–346.

Sinclair, H.D., Coakley, B.J., Allen, P.A. & Watts, A.B. (1991) Simulation of foreland basin stratigraphy using a diffusion model of mountain belt uplift and erosion: an example from the central Alps, Switzerland. *Tectonics*, **10**(3), 599–620.

Steckler, M.S. & Watts, A.B. (1978) Subsidence of the Atlantic-type continental margin off New York. *Earth Planet. Sci. Lett.*, **41**, 1–13.

Suppe, J. (1980) A retrodeformable cross section of Northern Taiwan. *Proc. Geol. Soc. China*, **23**, 46–55.

Suppe, J. (1981) Mechanics of mountain building and metamorphism in Taiwan. *Mem. Geol. Soc. China*, **4**, 67–89.

Suppe, J. (1984) Kinematics of arc-continent collision, flipping of subduction, and back-arc spreading near Taiwan. *Mem. Geol. Soc. China*, **4**, 67–90.

Tang, C.H. (1977) Late Miocene erosional unconformity on the subsurface Peikang high beneath the Chiayi-Yunlin coastal plain, Taiwan. *Mem. Geol. Soc. China*, **2**, 155–167.

Taylor, B. & Hayes, D.E. (1980) The tectonic evolution of the South China Basin. In: *The Tectonic and Geological Evolution of the Southeast Asian Seas and Islands* (Ed. by D.E. Hayes), pp. 89–104. American Geophysical Union, Washington, DC.

Taylor, B. & Hayes, D.E. (1983) Origin and history of the South China Sea Basin. In: *The tectonic and geologic evolution of Southeast Asian seas and islands* (Ed. by D.E. Hayes), pp. 23–56. AGU, Washington, DC.

Teng, L.-S. (1990) Geotectonic evolution of Late Cenozoic Arc-continent in Taiwan. *Tectonophysics*, **183**, 67–76.

Teng, L.-S. (1996) Extensional collapse of the Northern Taiwan mountain belt. *Geology*, **24**, 945–952.

Thorne, J.A. & Watts, A.B. (1989) Quantitative analysis of North Sea subsidence. *Am. Assoc. Pet. Geol. Bull.*, **73**(1), 88–116.

Ting, H.H., Huang, C.Y. & Wu, L.C. (1991) Paleoenvironments of the late Neogene sequences along the Nantzuhsien river, southern Taiwan. *Pet. Geol. Taiwan*, **26**, 121–149.

Tsai, Y.-B. (1986) Seismotectonics of Taiwan. *Tectonophysics*, **125**, 17–37.

Turcotte, D.L. & Schubert, G. (2002) *Geodynamics: Applications of Continuum Mechanics to Geological Problems*. Cambridge University Press, Cambridge.

Ussami, N., Shiraiwa, S. & Dominguez, J.M.L. (1999) Basement reactivation in the a Sub-Andean Foreland flexural bulge: the Pantanal Wetland, SW Brazil. *Tectonics*, **18**, 25–39.

Van Hinte, J.E. (1978) Geohistory analysis – application of micropaleontology in exploration geology. *Am. Assoc. Pet. Geol. Bull.*, **62**, 201–222.

Wang, W.-H. (2001) Lithospheric flexure under a critically tapered mountain belt: a new technique to study the evolution of the Tertiary Taiwan orogeny. *Earth Planet. Sci. Lett.*, **192**, 1571–1581.

Waschbush, P. & Royden, L. (1992) Spatial and temporal evolution of foredeep basins: lateral strength variations and inelastic yielding in continental lithosphere. *Basin Res.*, **4**, 169–178.

Watts, A.B. (1989) Lithospheric flexure due to prograding sediment loads: implications for the origin of offlap/onlap patterns in sedimentary basins. *Basin Res.*, **2**, 133–144.

Watts, A.B. (2001) *Isostasy and Flexure of the Lithosphere*. Cambridge University Press, Cambridge.

Yeh, M.G. (1987) Sedimentation of the Shangtao formation along the Wenshui-Chi, Miaoli. *Pet. Geol. Taiwan*, **23**, 87–113.

Yu, H.-S. & Chou, Y.-W. (2001) Characteristics and development of the flexural forebulge and basal unconformity of western Taiwan foreland Basin. *Tectonophysics*, **333**, 277–291.

Yu, S.-B., Chen, H.-Y. & Kuo, L.-C. (1997) Velocity field of GPS stations in the Taiwan area. *Tectonophysics*, **274**, 41–59.

Manuscript received 7 November 2005; Manuscript accepted 26 June 2006